Journal of Manufacturing Processes 133 (2025) 524–555

Contents lists available at ScienceDirect

Journal of Manufacturing Processes

journal homepage: www.elsevier.com/locate/manpro

Review article

A review on physics-informed machine learning for process-structure-property modeling in additive manufacturing

Meysam Faegh [a], Suyog Ghungrad [a], João Pedro Oliveira [b], Prahalada Rao [c], Azadeh Haghighi [a,*]

[a] Department of Mechanical and Industrial Engineering, University of Illinois Chicago, Chicago, IL, USA
[b] CENIMAT/I3N, Department of Materials Science, NOVA School of Science and Technology, Universidade NOVA de Lisboa, Caparica 2829-516, Portugal
[c] Grado Department of Industrial and Systems Engineering, Virginia Tech, Blacksburg, VA, USA

ARTICLE INFO

Keywords
Additive manufacturing
Physics-informed machine learning
Process-structure-property relationships
Physics-based feature engineering
Physics-based architecture
Physics-based loss function

ABSTRACT

This article presents a state-of-the-art review of the emerging field of physics-informed machine learning (PIML) models in additive manufacturing for process-structure-property modeling. Additive manufacturing processes hold immense potential for fabricating intricate and complex geometries across diverse applications and material classes. From a quality assurance standpoint, appropriate modeling of process-structure-property relationships of additive manufacturing processes using either physics-based or machine learning (ML)-based approaches has been a topic of intensive research. As an example, ML of data acquired from in-situ sensors is related to flaw formation, e.g., porosity, cracking, or deformation. In recent years, the computational burden of pure physics-based models, the large data set requirement, and their black-box nature, i.e., the lack of interpretability of ML models, have prompted researchers to turn to PIML models. In PIML models, physical insights of the additive manufacturing process gained from various means are integrated with ML models, resulting in a more robust and interpretable framework for both process and microstructure evolution. A key delineator is the source of physical knowledge to be fused into PIML models, which can be obtained either from governing physical equations, data-centric feature extraction without implementing any physical equations, or a hybrid of the two foregoing. Within this review, we stratify PIML models based on the method used for the fusion of physical knowledge to ML models, into three categories, namely: (i) physics-based feature engineering, (ii) physics-based architecture shaping of ML models, and (iii) physics-based modification of the loss function of the ML models. For each of these categories, we further delineate the source of physical knowledge, ML models, integration approach, and data-set requirement, among others. A comparative analysis of the reviewed studies is presented and critically discussed, while the potential research gaps, along with future research directions on developing PIML models for different AM technologies are outlined.

1. Introduction

1.1. Motivation and rationale

Additive manufacturing (AM) allows for the direct transformation of digital designs into physical objects through layer-by-layer deposition, joining, or solidification of materials without the need for molds, tools, or extensive manual labor [1]. In comparison with conventional manufacturing techniques, AM offers numerous advantages, including the ability to manufacture intricate, complex, and customized geometries at a significantly reduced cost, minimizing production time-to-market, and realization of novel material compositions and designs with tailored functionalities [2]. Additionally, AM has demonstrated significant potential in reducing the carbon footprint and enhancing process efficiency by reducing scrap rates and material waste and eliminating the need for assemblies, resulting in a simplified manufacturing process [3–5].

Given its numerous evolving capabilities, AM has transformed from a mere prototyping technique into a highly promising technology solution across various industries and sectors, including aerospace [6], energy [7], and healthcare [8]. With this growing industrial adoption and interest, AM product certification and qualification through characterizing the process-structure-property (PSP) relationships has been a significant focus of research [9–11]. Process-structure-property modeling involves understanding and predicting the relationships between AM process

* Corresponding author.
E-mail address: ahaghi3@uic.edu (A. Haghighi).

https://doi.org/10.1016/j.jmapro.2024.11.066
Received 10 June 2024; Received in revised form 23 October 2024; Accepted 22 November 2024
Available online 30 November 2024
1526-6125/

Abbreviations

AM	Additive manufacturing
ANN	Artificial neural networks
CNN	Convolutional neural networks
DACM	Dimensional analysis conceptual modeling
DED	Directed energy deposition
DT	Decision trees
ETR	Extra trees regressor
FEM	Finite element method
GAN	Generative adversarial networks
GB	Gradient boosting
GNN	Graph neural network
GPR	Gaussian process regression
KNN	K-nearest neighbors
LINREG	Linear regression
LOGREG	Logistic regression
LSTM	Long short-term memory
MEX	Material Extrusion
ML	Machine learning
PBF	Powder bed fusion
PCA	Principal component analysis
PDE	Partial differential equations
PIDL	Physics-informed deep learning
PIML	Physics-informed machine learning
PINN	Physics-informed neural network
PSP	Process-structure-property
RGNN	Recurrent graph neural network
RF	Random forest
RMSE	Root mean square error
RNN	Recurrent neural networks
SHAP	Shapley additive explanation
SVM	Support vector machine
SVR	Support vector regression
VAE	Variational autoencoders
VPP	Vat photopolymerization

parameters and signatures, the microstructure of the printed material, and the resulting micro to macro-level properties (e.g., mechanical performance, dimensional accuracy), e.g., as shown in Fig. 1 for PBF process, towards process optimization, tuning, and control for achieving customized properties. Due to the complex underlying multi-scale and multi-physics phenomena in AM, establishing the PSP relationships is a challenging task and thus, both experimental and theoretical approaches have been considered by researchers.

Experimental techniques are frequently used to study various parameters related to the AM process, microstructural defects [12], mechanical properties [13], dimensional accuracy [13] and geometric features [14] of printed parts. The experimental techniques cover a wide range of ex-situ and in-situ methods, such as electron microscopy [15], X-ray computed tomography [16], infrared thermography [17] and ultrasound [18]. Despite the potential advantages of experimental approaches for validation purposes and providing valuable insights, they often require extensive setup preparation, are time-consuming and costly, and may be hard to generalize since the results may not reflect the entire parameter space of the AM process. On the other hand, analytical and numerical models based on process physics may be adopted for multi-scale modeling and simulation of various complex phenomena in AM processes such as analytical modeling of fusion zone dimensions [19] and scanning strategy impact on temperature field in PBF [20], multiphysics modeling to discover PSP-relationships in fusion-based metal AM [21], grain growth in electron beam AM [22], powder gas interaction in LPBF [23], melt pool signatures in PBF [24], degree of cure in stereolithography AM [25], clad characteristics in DED [26], and microstructure evolution [27]. Comprehensive reviews of numerical modeling approaches within the field of AM have been done in [28–30].

Although physics-based models play an important role in revealing the underlying mechanisms of AM processes, they often pose a significant drawback due to their time-consuming nature, complexity, and their high computational costs [31–40]. As a result, they offer limited practicality for on-the-fly decision-making [41]. Additionally, these models might fail to fully capture the process variations and uncertainties, due to various approximations and unknown parameter assumptions, leading to limited scalability and generalizability. To address these challenges, data-driven and machine learning (ML) models have become extremely popular in the AM community for PSP modeling, defect detection, and quality control [42–45]. Through seamless integration of various digital systems and sensors with the AM setup, ML models can readily access the necessary data of various modalities [46] and have shown significant promise in revealing hidden patterns and relationships, when provided with appropriate data [47]. Additionally, ML models can be leveraged to enhance existing physical models. For example, Haghighi and Li [48] applied ML techniques to improve the accuracy of a physical bonding model used in material extrusion (MEX). In their approach, they first used an ML model to map experimental data to deformations. Then, based on these ML-predicted deformations, they developed a geometric model that refined the original physical bonding model, resulting in improved predictions.

Despite their significant potential, ML-based approaches for PSP modeling generally rely on massive high-quality datasets to generate reliable, accurate, and high-fidelity results. Additionally, measuring certain critical aspects of AM processes can be highly challenging, if not impossible. For example, in the powder bed fusion (PBF) process, key parameters such as melt pool velocity, temperature gradients, melt pool depth, and the sub-surface solidification front are particularly difficult to measure [49]. This becomes a significant challenge in the context of AM, given the costly nature of data acquisition and processing due to the process's slow print speed and the limited data resulting from mass customization. Furthermore, ML models lack the ability to provide physical insights and explanations for their predictions due to their black-box nature, which may be critical to AM practitioners and researchers, hindering its potential industrial upscaling. Consequently, this lack of interpretability will adversely affect the model's trustworthiness in critical AM applications [50].

The evolving AM paradigm requires PSP models to possess several key attributes [51]. These include rapidity, generalizability, scalability, and transferability across diverse AM processes, machines, geometries, and materials, all while maintaining accuracy under various processing conditions. To help tackle these challenging requirements, a promising solution has emerged in the form of physics-informed machine learning (PIML) models, which fuse physical knowledge with ML techniques. PIML models, often referred to as gray-box models, present a promising solution by combining the advantages of white-box physics-based models with those of black-box ML models. They help reduce the computational intensity seen in traditional physics-based models and alleviate the data demands and interpretability issues often faced by black-box ML models [52,53]. Though not fully interpretable, PIML models provide a more transparent alternative to black-box methods due to the fusion of physical knowledge into the model [54–56].

Researchers have explored various approaches to fuse physical knowledge with ML models, as shown in Fig. 2, including fusion during input data preparation, ML model design and selection, as well as ML model training, evaluation and tuning, each offering unique promises and challenges. Additionally, valuable physical or domain-knowledge insights can be extracted from diverse sources, such as governing

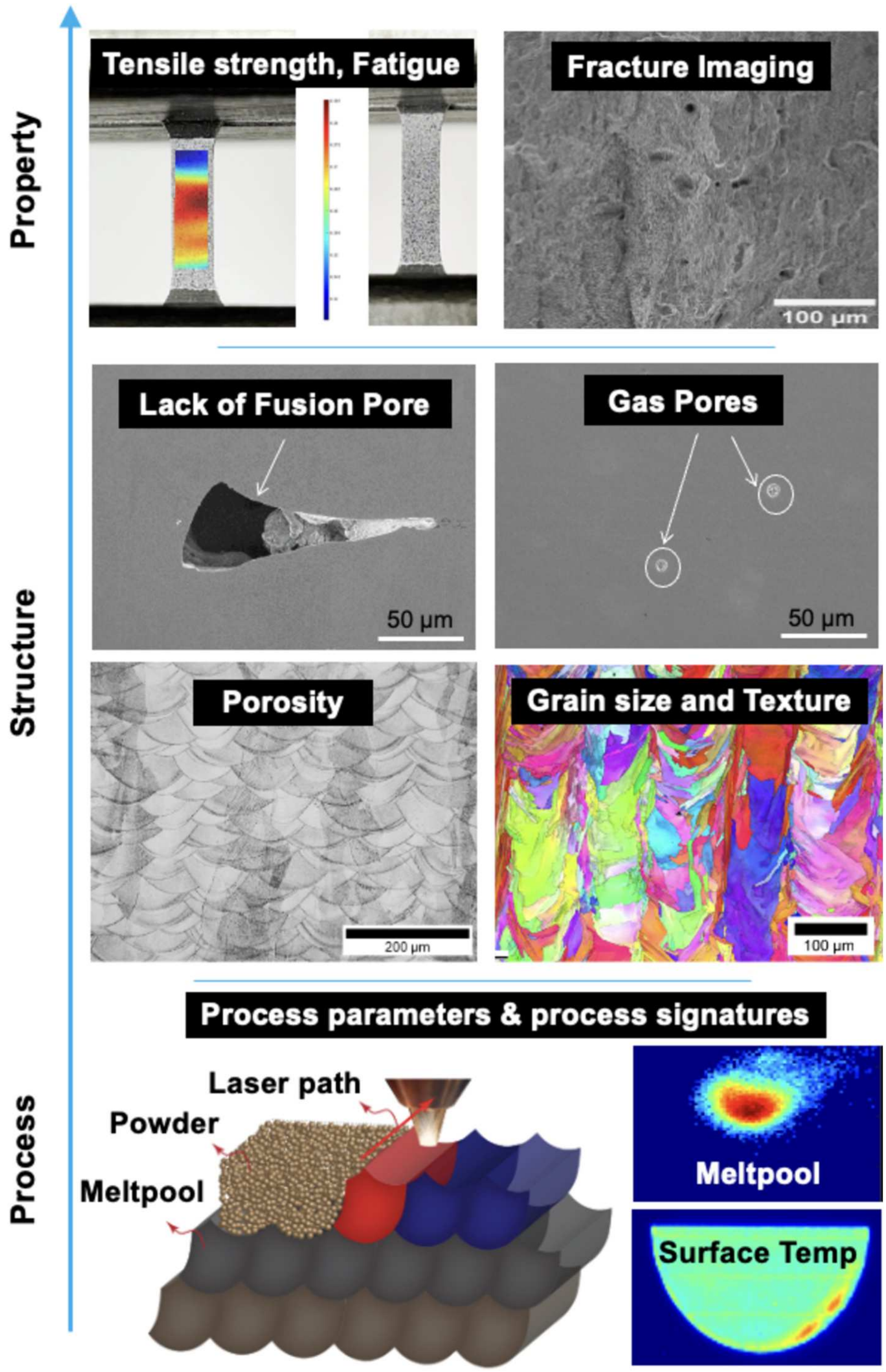

Fig. 1. Process-structure-property relationships.

physical equations, data-centric approaches, or a hybrid combination of the two. To pave the way for future research on PIML for PSP modeling in AM, comprehending the current state-of-the-art research becomes imperative. Current review papers tend to emphasize metal AM processes, often overlooking other AM technologies [57–61]. Additionally, with the recent wave of PIML studies, many crucial aspects of these models have not been thoroughly examined in earlier reviews. This study aims to bridge that gap by providing an extensive review of the most up-to-date PIML approaches for PSP modeling in AM. It will offer new perspectives on the sources of physical knowledge as a key delineator among PIML models, explore the latest physics fusion techniques, and critically assess the capabilities, limitations, and practical applications of different PIML models, while identifying research gaps and future directions for advancement.

1.2. Approach

We employ the following two primary criteria (among other factors) to classify the diverse PIML approaches in the AM literature for PSP modeling:

(1) ***Source of physical knowledge:*** This criterion addresses the origin of the physical knowledge used in the models, elucidating its

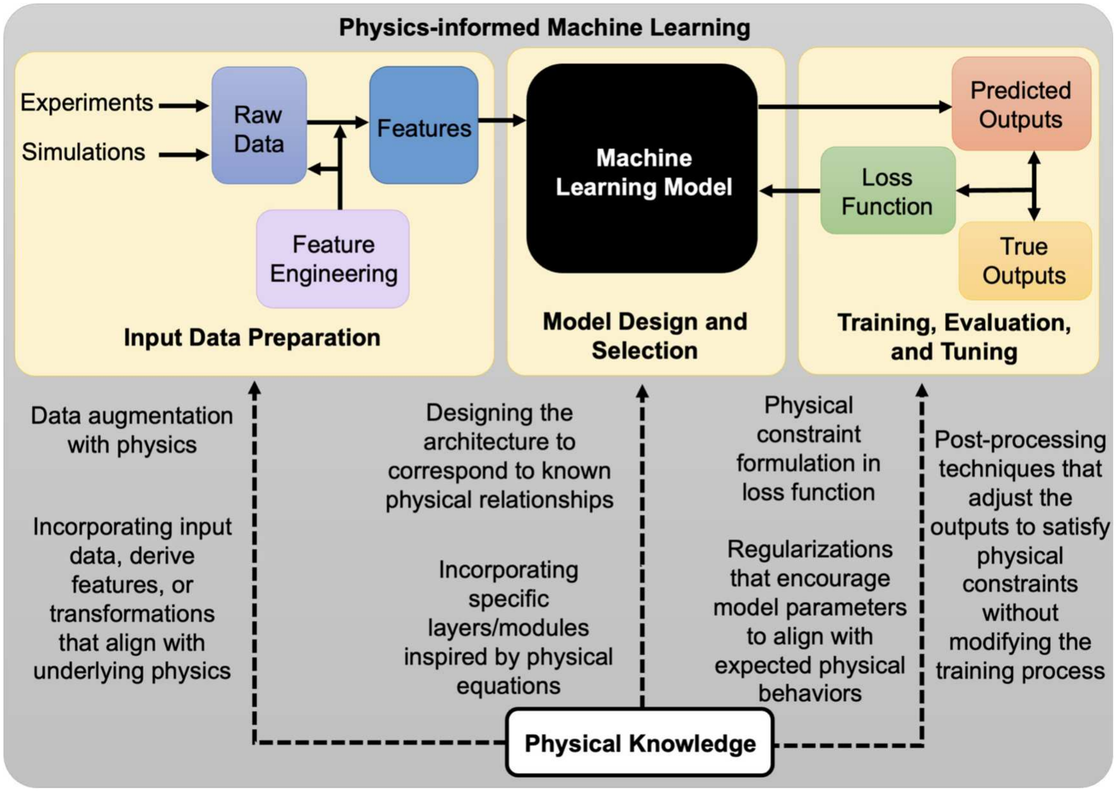

Fig. 2. Overview of the PIML concept.

origins and whether it arises from empirical data, analytical equations, or physical simulations.

(2) ***Fusion method:*** This criterion addresses how physical knowledge is effectively integrated into ML models, elucidating the mechanisms employed to combine the insights from physics with the predictive capabilities of ML algorithms.

As depicted in Fig. 3, physical knowledge essential for PIML models can be derived from different sources and integrated into various components of the machine learning models. These sources of physical knowledge encompass three main categories:

(i) Governing physical equations, i.e. explicit mathematical representations of the underlying physics in terms of partial differential equations (PDEs), physical laws, empirical relationships, among others, which can be either directly fused into ML architecture or loss function and solved while training the network, or they can be integrated through the solutions obtained from analytical approaches or numerical simulations as PIML inputs,
(ii) Data-centric methods, such as statistical techniques and image analysis methods, which extract relevant and important physical parameters or information as well as explainable terms directly from the data without relying on explicit physical equations, and
(iii) Hybrid methods that combine both sources of physical knowledge above, leveraging the strengths of both physics-based equations and data-driven methods to achieve a more robust and accurate characterization of the underlying physical processes.

Additionally, per Fig. 3 we consider three main approaches for the fusion of physical knowledge into ML models:

(i) Physics-based feature engineering, which deals with leveraging physical knowledge to form the ML model input, i.e., fusion during input data preparation for any ML model,
(ii) Physics-based architecture shaping, which deals with leveraging physical knowledge to ML model design and parameter formulation, including but not limited to the design of layers, nodes, tree connections, weights, biases, activation, learning rates, similarity metrics, and kernel functions, i.e., fusion during model design and selection for any ML model,
(iii) Physics-based loss function modification, which deals with leveraging physical knowledge during ML model training and testing by directly incorporating them into the ML model loss function (not limited to only neural networks), i.e., fusion during model training, evaluation and tuning for any ML model.

In this comprehensive and critical review, we initially focus on the second criterion to classify the existing PIML literature into three main groups based on the fusion method of the physical knowledge into the ML model, namely (1) Physics-based feature engineering, (2) Physics-based architecture shaping, and (3) Physics-based loss function modification. Subsequently, within each category, we delve into various intricate aspects, including the source of physical knowledge, the specifics of ML model and physics integration, leading to the formation of distinct subclasses. Finally, to present a concise overview, the studies associated with each of the aforementioned classes (1)-(3) are thoughtfully summarized in a structured table, facilitating a clear understanding of the diverse approaches and findings in this field.

1.3. Paper selection criteria

A thorough online literature search was performed across Google Scholar and Web of Science. This search utilized a selection of specific keywords and phrases, including: (physics-informed or physics-based or physics-aware or physics-driven or physics-guided or scientific or

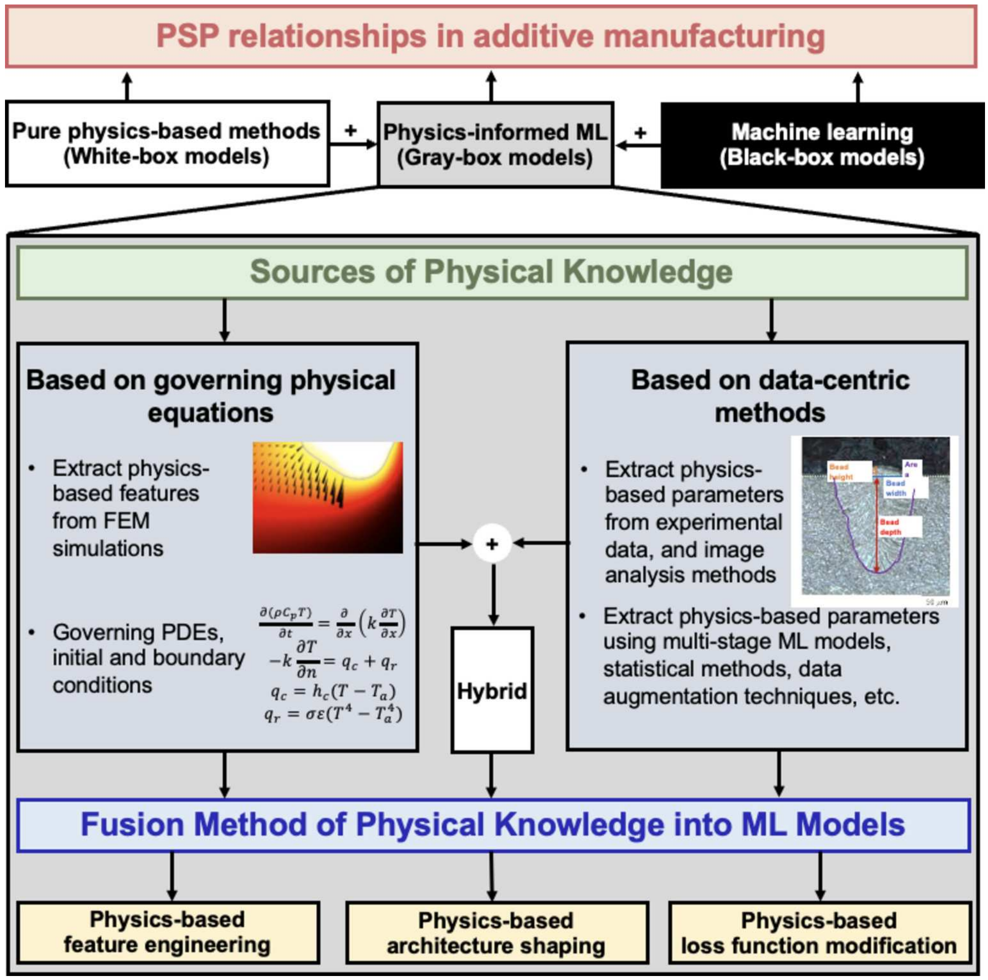

Fig. 3. Overview of methods used for capturing process, structure, and property relationships in AM.

mechanistic or model-based or knowledge-based AND machine learning or deep learning or neural network or artificial intelligence AND additive manufacturing or material extrusion or fused filament fabrication or powder bed fusion or directed energy deposition or binder jetting or material jetting or sheet lamination or vat photopolymerization or stereolithography). All these keywords were thus utilized to identify relevant research papers in the current study. However, to maintain simplicity and coherence, this study employs the term PIML, which encompasses all such approaches that fuse physics into a wide variety of machine learning models, spanning from classical ML to deep neural networks. Moreover, this review specifically focuses on process-structure-property modeling in AM and any of its sub-chains, namely process-structure modeling, process-property modeling, or structure-property modeling. Therefore, any PIML studies in the field of AM beyond this scope, e.g., solely associated with material or particle distribution design as well as topology optimization, are excluded from this review.

In Section 2, an overview of various AM technologies and ML models is provided. Section 3 classifies the PIML studies for PSP modeling in AM, into various subgroups based on the proposed approach earlier by leveraging factors such as the fusion method and source of physical knowledge among others, and provides a detailed description of the existing literature. Next, in Section 4, a comprehensive analysis of all reviewed PIML studies is outlined, and research gaps, as well as potential future research directions are highlighted. Finally, concluding remarks are summarized in Section 5.

2. Overview of additive manufacturing technologies and machine learning models

This section provides a brief overview of various AM technologies and ML models that are often used in the context of PSP modeling, serving as a valuable point of reference throughout this review and providing essential insights for the reader.

2.1. Additive manufacturing technologies

Additive manufacturing technologies work on the principle of adding material generally in a layer-by-layer fashion. There are seven main categories of AM defined by ISO/ASTM 52900 standard [62]: binder jetting, directed energy deposition (DED), material extrusion, material jetting, powder bed fusion, sheet lamination and vat photopolymerization (VPP). Table 1 provides an overview of these AM technologies and their working principle. Additional details on these processes, their capabilities, material compatibility, and their advantages/disadvantages may be found in [1].

2.2. Machine learning models

The ML methods used for PSP modeling in AM can be categorized into classical ML and deep learning models, as shown in Table 2 [75]. Classical ML models are comprised of a variety of ML methods, from regression-based parametric models and support vector machines (SVM) to non-parametric methods (e.g., Gaussian process regression (GPR), K-nearest neighbors (KNN)) and tree-based models. In addition to the

Table 1
Overview of AM processes.

AM process	Working principle	Illustration
Binder Jetting	A binder liquid is used to join powdered material. The parts are heated to cure the binder and then de-powdered and sintered to get the desired level of properties [34].	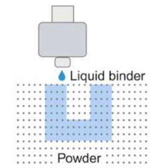
Directed Energy Deposition	Focused thermal energy (e.g., laser, electron beam, electric arc, plasma arc) is used to melt and fuse material (either in the from of powder [63] or wire [64]) that are simultaneously deposited [65].	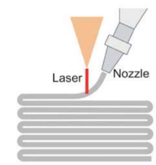
Material Extrusion	Molten material (e.g., in fused deposition modeling [66] and fused filament fabrication [67]), or viscous paste or ink-based solutions (e.g., in electrohydrodynamic jet printing [68], or continuous direct ink-writing) is extruded and selectively deposited as a continuous stream through a nozzle [69]	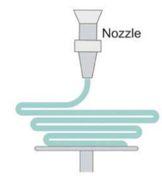
Material Jetting	Controlled drops of inks are ejected from the printhead nozzles onto a substrate and get dispensed and coalesced [70].	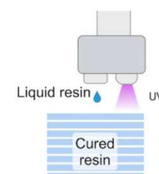
Powder Bed Fusion	An energy source (e.g., laser, electron beam) is used to bind through melting (e.g., in electron beam melting and selective laser melting) or sintering (e.g., in selective heat sintering, selective laser sintering, and direct metal laser sintering) of powder particles within a bed of powder [71,72]	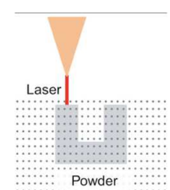
Sheet Lamination	Metallic sheets are used as feedstock and fused together through a laser or ultrasonic energy source [73].	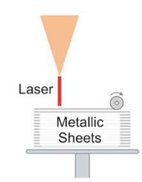
Vat Photopolymerization	A liquid photopolymer resin within a vat is selectively cured or solidified using a light source, such as a UV laser (e.g., stereolithography) or a digital light projector [74].	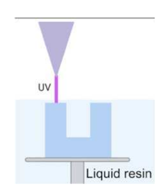

various classical ML models, deep learning models, which are ML models based on neural networks, are also frequently explored in PSP modeling [76]. Among the different types of deep learning models are artificial neural networks (ANN), convolutional neural networks (CNN), graph neural networks (GNN), and recurrent neural networks (RNN). For brevity, an overview of the most common and foundational techniques in ML, which are also used in PIML modeling of AM processes are summarized in Table 2 [75].

A wide variety of unique neural networks with distinct characteristics and variations, such as self-organizing maps [77] and spiking neural networks [78] have been studied in recent years. Furthermore, different ML models are combined in sophisticated ways to create more advanced deep learning architectures such as generative adversarial networks (GAN) [79], variational autoencoders (VAEs), attention mechanisms, and deep belief networks, among others. For instance, two ANNs can be integrated or combined together to form VAE (i.e., encoder-decoder architecture), where the encoder is the first ANN that encodes inputs into a fixed-length internal representation and the decoder is the second ANN that uses this representation to make predictions. Encoder-decoder methodologies have frequently been explored in the context of PSP modeling in AM, such as for anomaly detection [80] and heat map prediction [81].

All ML approaches discussed above generally follow a similar procedure; first, data is derived from either experimental observations or

Table 2
Overview of ML models.

Method	Main remarks
Classical ML models	
Gaussian process regression	A non-parametric ML approach that models the relationship between input variables and output values as a probability distribution over functions. Instead of assuming a fixed function form, GPR uses a prior distribution based on observed data and updates it to a posterior distribution as new data is incorporated, allowing for flexible and accurate predictions while providing uncertainty estimates.
K-nearest neighbors	A non-parametric method for regression or classification tasks which relies on the similarity of the new data point to its k-nearest neighbors in the training dataset for prediction.
Regression-based parametric models	Parametric ML models that make explicit assumptions about the functional form of the relationship between the input and output, e.g., linear relationship in linear regression and non-linear relationships via higher-degree polynomial terms in polynomial regression. The most common models are linear regression (LINREG) for regression tasks and logistic regression (LOGREG) for classification tasks.
Support vector machines	Models that transform the data into higher dimensions using kernel functions and then identify a hyperplane where the data can be linearly separated. If they are used for regression applications, they are called support vector regression (SVR).
Tree-based models	Graphical representation of decision rules in tree-like structures, where each node corresponds to a decision or feature, and each branch represents a possible outcome or decision. Some popular tree-based models are decision trees (DT), gradient boosting (GB), and random forest (RF).
Deep learning models	
Artificial neural networks	The basic form of neural networks which consists of inputs, outputs, and one or more hidden layers of fully connected neurons [82]. Deep neural networks and multilayer perceptron neural networks are also considered as ANNs with more than one layer. For simplicity, all the above names have been considered ANN in this review.
Convolutional neural networks	A type of neural network used for image and video processing [83]. An important part of CNN is the convolutional layer, which applies a set of kernels or filters to the input image to extract features. Another important part is the pooling layer, which downsamples the feature maps to reduce spatial dimensions and computational cost. The final layer in CNN generally takes the flattened feature maps as inputs and makes predictions.
Graph neural networks	Deep learning architectures that capture the relationships in unstructured graphs by message passing between neighboring nodes [84].
Recurrent neural networks	Neural network models that can process sequential data and temporal problems. They can handle inputs of variable lengths and keep a memory of past inputs to influence the output of the current time step. Some popular RNN variants are long short-term memory (LSTM), vanilla RNN, gated recurrent unit, and bidirectional RNN.

simulations and then goes through a data preparation/feature engineering step before being fed into the ML model architecture. The loss function serves as the evaluator of the model's performance, guiding the model's optimization until the threshold of a predefined and desired criterion is obtained. Physics-informed machine learning follows a similar trend to machine learning models; however, additional knowledge from physics is fused to the different stages of the machine learning model, from input data preparation and feature engineering to model architecture design and loss function modification. Therefore, the key distinction among various PIML approaches lies in the timing/stage of physics integration. i.e., the ML stage, in which physical knowledge is fused. Additionally, one may consider the source of physical knowledge as a secondary criterion to categorizing various PIML models, as considered in this work.

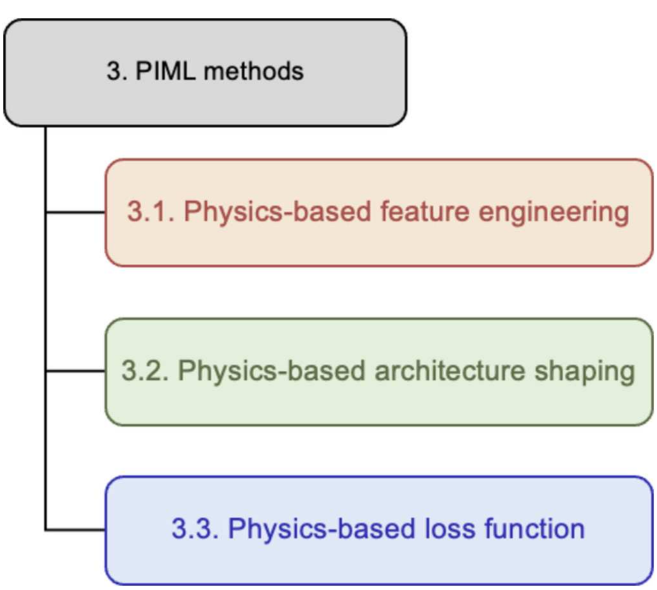

Fig. 4. Categorization of the reviewed PIML methods in terms of physics fusion.

3. PIML methods

In this section, a comprehensive review of various PIML models developed for PSP modeling in different AM technologies is presented, and both the source of physics and integration/fusion method, among other factors such as the focused AM technology and adopted ML model, are critically discussed. As shown in Fig. 4, the primary criterion for classification in the current review is the fusion method/stage, forming three distinct classes of (1) Physics-based feature engineering, (2) Physics-based architecture shaping, and (3) Physics-based loss function modification.

3.1. Physics-based feature engineering in PIML models

Feature engineering refers to the process of selecting, manipulating, and converting raw data or features into formats that correspond more closely with the intended outcome for ML models. If executed properly, feature engineering can enhance the worth of the available data, enhance ML model effectiveness, decrease data complexity, and eliminate unnecessary and irrelevant features. Conversely, incorporating poor-quality features may necessitate constructing more intricate models to achieve comparable performance levels.

Physics-based feature engineering involves the strategic construction and selection of input features that not only encapsulate the raw data's characteristics but also integrate domain-specific knowledge derived from underlying physical principles. This approach seeks to enhance the model's performance, robustness, and interpretability by enriching the feature set with information rooted in physics. For example, one may consider incorporating physical variables as features or consider retaining the most informative physical components during the dimensionality reduction steps. Additionally, physics-based transformations to raw data may enable capturing underlying physical behaviors and extracting time-related features can encapsulate temporal patterns that align with the system's physics. Finally, data augmentation can be considered using the underlying process physics to increase the size of raw data or reveal interaction terms between different physical variables that may influence the system.

As shown in Fig. 5, we summarize the various techniques used for physics-based feature engineering into three subclasses based on the source of the physical knowledge, namely (i) physics-based feature engineering based on governing physical equations, (ii) physics-based feature engineering based on data-centric methods such as feature extraction/selection using statistical methods, image data analysis and multi-stage machine learning models and (iii) a combination of equation-based and data-centric feature engineering approaches. Table 3 reports a summary of the literature employing physics-based feature engineering for constructing PIML models towards PSP modeling in AM. Additional details on these studies are further discussed in the following subsections.

3.1.1. *Physics-based feature engineering based on governing physical equations*

This category explores the application of already established governing physical equations and explicit theoretical/physical models during the feature engineering step and can be further classified into three sub-groups depending on the adopted approach, i.e., (i) dimension augmentation using numerical approaches, (ii) dimension augmentation using analytical approaches, and (iii) data augmentation based on process physics. Dimension augmentation involves incorporating additional physics-based features as inputs in PIML models. In contrast, data augmentation focuses on expanding the dataset's size by generating more data points without altering the original types of input features used.

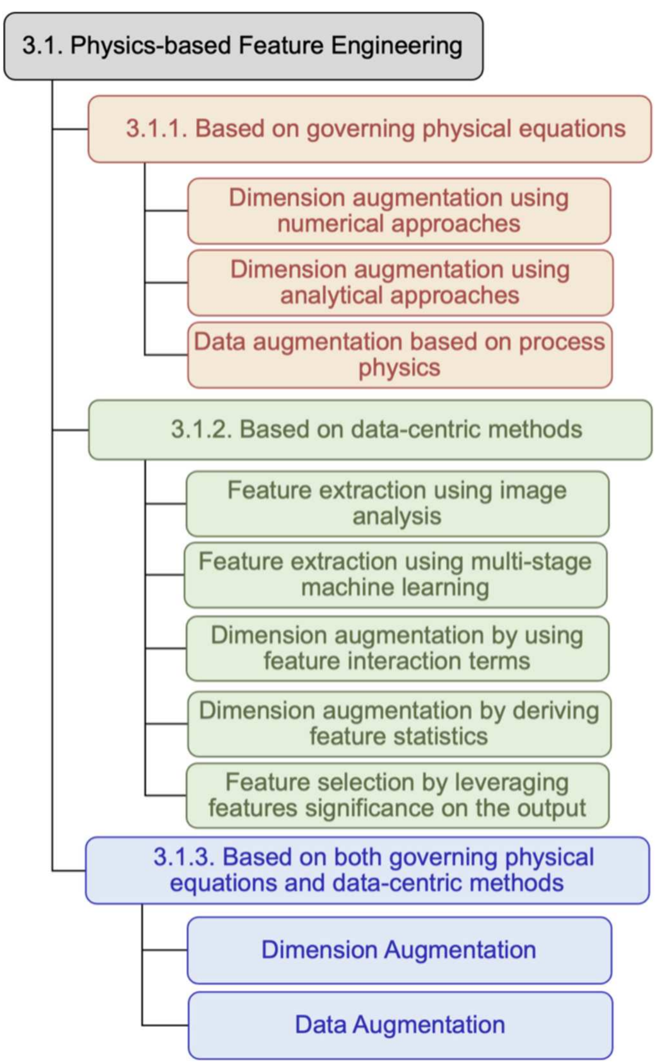

Fig. 5. Categorization of the reviewed PIML methods based on physics-based feature engineering.

(i) Dimension augmentation using numerical approaches

Numerical approaches, focused on solving/simulating real-world phenomena by approximating solutions through computation, may be used to generate/augment new important physical variables or features based on the underlying process physics as ML model inputs to build PIML models.

Du et al. [85] proposed that the physics behind the defect formation in the PBF process can be revealed by six mechanistic variables. These variables, namely volumetric energy density, Marangoni number, solidification time of the pool, surface tension force, Richardson number, and molten pool aspect ratio (pool length/depth), were computed by a mechanistic model and used as inputs of PIML model to predict the occurrence of balling defect (Fig. 6). A balling susceptibility index was derived from the experimental ball formation data and their corresponding mechanistic variables using a genetic algorithm. The index is validated and tested using a 166 set of available data from the literature, with a minimum classification error threshold. The introduced index predicted balling defects with 90 % accuracy. Additionally, the researchers utilized ML indices such as information gain, information gain ratio, and Gini index to determine the hierarchical importance of the mechanistic variables in the formation of defects. It was discovered that the Marangoni number and solidification time had the greatest influence on balling, with the former being the most significant and the latter coming in second place. Guo et al. [92] integrated a high-fidelity powder-scale mechanistic model of the PBF process with PINN. Mechanistic variables (dimensionless peak temperature, Richardson number, ratio of recoil pressure and surface tension, solidification time, and Fourier number) were related to the printing quality using a quality prediction index. Eventually, the hierarchy importance of the mechanistic variables was determined.

Mondal et al. [86] studied the impact of solidification stress, cooling rates, the ratio of the vulnerable and relaxation times, and the ratio of the temperature gradient to the solidification growth rate on the physics of cracking in a PIML framework for the PBF process. The physics-based variables were calculated using a mechanistic modeling approach and fed into a PIML model to predict crack formation, which may be more prone to occur in certain alloy systems. It was reported that the solidification stress has the greatest influence while the cooling rate has the least influence. The performance of the SVR, DT, LINREG, and LOGREG models was investigated, and accuracy levels were 90.2 %, 85.3 %, 84.3 %, and 70 %, respectively. To develop a PIML method for microstructure evolution, Riensche et al. [93] developed a PIML model to predict two microstructure characteristics, i.e., meltpool depth and primary dendritic arm spacing in PBF. A rapid part-scale thermal model was utilized to estimate the sub-surface end-of-cycle temperature and cooling rate. Then, based on the physics-based thermal history quantifiers obtained from the thermal model, an SVM model was trained. Root mean square error (RMSE) for the meltpool depth and primary dendritic arm spacing was obtained as 12 μm and 70 nm, respectively.

Using thermo-fluid flow simulations, Kats et al. [87] created a PIML model that can recognize the connection between the characteristics of the local thermal features and the grain structure. To generate the required data for training the neural network, the thermal data and grain structure characteristics were calculated using the finite volume method and cellular automaton method, respectively. The deposited material domain was split into a set of cuboids. The thermal gradient and cooling rate at 8 positions inside the cuboids are used as inputs, while the local average grain size or average aspect ratio of the grains within the cuboid are considered as outputs. For a dataset comprised of both single-layer and multi-layer builds of DED Inconel 718, the coefficient of determination was more than 0.95. It was concluded that the proposed

Table 3
Summary of studies on physics-informed feature engineering based on a. governing physical equations, b. data-centric extraction, c. both physical equations and data-centric extraction.

Ref	Year	AM process	ML method	Integrated physical knowledge	Dataset size	Target
a. Source of physical knowledge based on governing physical equations						
[85]	2021	PBF	LINREG	Mechanistic variables calculated using a heat transfer and fluid flow model	166	Balling defects
[86]	2022	PBF	DT, LINREG, LOGREG, SVR	Heat transfer and fluid flow model	102	Crack formation
[87]	2021	DED	ANN	Physical relationship of the grain structure and thermal conditions	1242	Grain structure characteristics
[88]	2021	PBF	LINREG, GPR, SVR	Physical equations for energy density distribution and pressure distribution	549	Pore diameter, pore spacing
[89]	2022	PBF	CNN	Semi-analytical heat transfer model with scan pattern information	–	Melt pool depth and volumetric fraction of grains
[90]	2023	DED	ANN, SVR	Fatigue crack growth life by the Paris' law	–	Fatigue life
[91]	2023	PBF	ANN	Equations of mass, momentum, and energy	103	Process parameters, width, and depth of meltpool
[92]	2023	PBF	DT	Fluid flow conservation equations	–	Build quality
[93]	2024	PBF	LINREG, LOGREG, SVM	Graph theory thermal modeling	1250	Meltpool depth and primary dendritic arm spacing
b. Source of physical knowledge based on data-centric extraction						
[94]	2022	PBF	LOGREG, KNN, SVM	Meltpool and ejecta features	22,400 images	Porosity type and severity classification
[95]	2018	PBF	SVR-PCA	Meltpool, plume, and spatter features	3318	Process quality level represented by track width level
[96]	2021	DED	CNN	Wavelet transform for CNN, Feature extraction using RF	12 experiments	Ultimate tensile strength, yield strength, and elongation
[97]	2020	PBF	ANN	Physics-based and statistics-based knowledge from sensor data	1009	Quality assurance
[98]	2021	PBF	ANN, DT, GPR, LINREG, RF, SVM	Physics-based analytical model and FEM simulations	5 simulations	Meltpool size
[99]	2022	MEX	ANN, RNN	Derive empirical models from domain knowledge	1273, 3000	Optimal print parameters
[100]	2022	PBF	ANN, SVM, RF	Meltpool peak temperature, Marangoni flow as physics-based inputs, and dimensionality augmentation of process parameters	110	Surface roughness, Relative density
[101]	2024	DED	GAN, RNN	Heat source as the forward diffusion process of diffusion models and autoencoders for feature extraction	–	Product properties
[102]	2024	PBF	LSTM	Process parameters, sequential information such as layer number, and section order and statistical features of emission	–	Section-wise thermal characteristics
[103]	2024	DED	ANN, KNN, LINREG, RF, SVM	Meltpool dimensions and temperatures from the simulation	99	Meltpool morphology
[104]	2024	PBF	GAN	Process parameters as domain knowledge for a generative model	2160	Sequential thermal history images
[105]	2023	DED	GAN-CNN	Using shape and temperature distribution of the melt pool and a control chart to perform data augmentation	–	Porosity
[106]	2023	DED	ANN	Partial derivatives as physics-based parameters related to the tensile strength, SHAP	135	Ultimate tensile stress, Yield stress
[107]	2023	PBF	ANN, RF, SVR	Stochastic parallel particle kinetic simulator, SHAP	960	Chord length distributions
[108]	2024	PBF	RF, GPR, KNN, ETR	SHAP analysis of atomic features	–	Melt pool depth
c. Source of physical knowledge based on both governing physical equations and data-centric extraction						
[109]	2020	DED	CNN	FEM simulation	1557 images	Pore occurrence, Pore size
[110]	2021	DED	GB	FEM for capturing the meltpool's temperature shape profile, Functional PCA	1564	Porosity prediction
[111]	2022	MEX	GPR	Five ODEs comprised of continuity, momentum, charge, electric field, energy, and constitutive equations	12 videos	Jet process dynamics
[112]	2023	MEX	SVR	Conservation and constitutive laws	100	Road width
[113]	2023	PBF	ANN, DT, KNN, LOGREG, RF, SVM	Signatures of the meltpool extracted from in-situ optical meltpool images	12 scan tracks	Keyhole pore prediction
[114]	2022	PBF	SVM, RF	Continuous damage mechanics based feature engineering	89	Fatigue life
[115]	2024	DED	CNN	Thermal image during deposition with analytical equation (Goldak heat flux)	–	Thermal history Surface deformations
[116]	2024	PBF	DARN	Using kullback-leibler divergence method for combining thermal-fluid simulation data with experimental data	50,000 data points	Normalized energy density, heat source depth, and heat source radius

approach could serve as a complementary technique to the 3D cellular automaton method to predict the grain structure in real time for large scale AM processing. In [103], simulating the DED process led to an assessment of the meltpool's shape, which was then utilized as data for a machine learning model to forecast the type of defects.

(ii) Dimension augmentation using analytical approaches

Analytical approaches, focused on deriving mathematical relationships between physical variables based on established mathematical principles, and semi-empirical relationships may be used to generate/

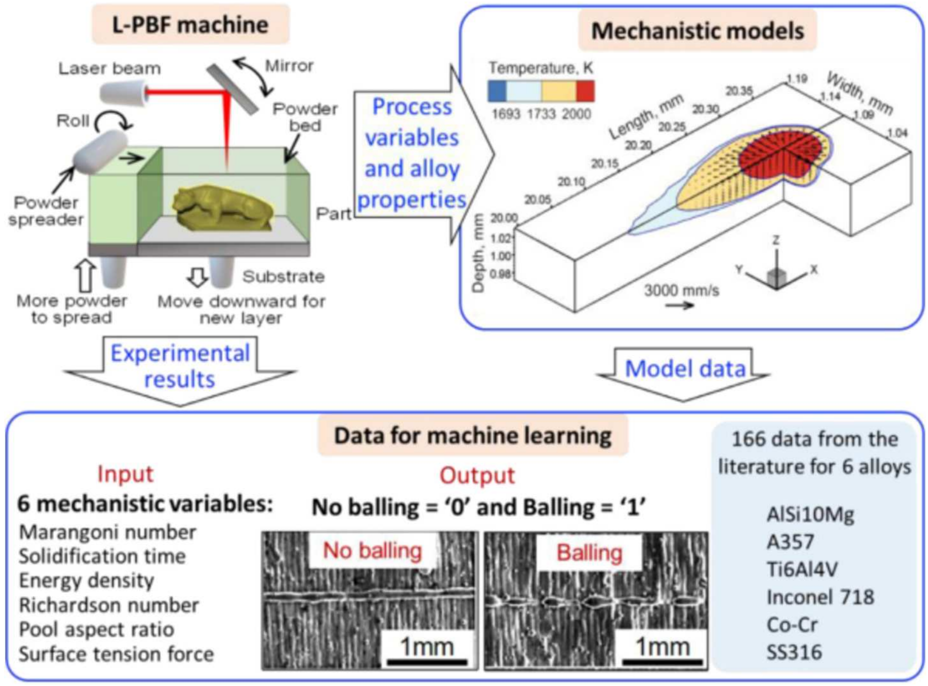

Fig. 6. Feature engineering based on governing physical Eqs. [85].

augment new important physical variables or features based on the underlying process physics as ML model input to build PIML models.

Following a theoretical approach, Liu et al. [88] proposed a PIML method for predicting pore generation in the PBF process. First, the machine setting parameters are used to theoretically calculate machine-independent physical effects such as energy density and radiation pressure of the laser. Then, these physics-based effects were used as model inputs to predict porosity level based on the pore maximum diameter. Linear regression, GPR, and SVR models with linear, Gaussian, radial basis function, and polynomial kernels were considered as machine learning models, and it was reported that the SVR with radial basis function outperforms the other models with a 13 % average error. Moreover, a conventional model that is dependent on the machine settings is compared to the PIML model. Results indicated that the machine independent PIML model has only 3 % accuracy deviation from the conventional model and has the potential to be used in various machines. Finally, a series of physics-porosity maps are provided to visualize and discuss the relationship between extracted physical effects and porosity. A semi-analytical model is used to generate temperature values for randomly produced scan patterns, which serve as inputs to a CNN for predicting the volumetric fraction of grains and the maximum melt pool depth [89]. Based on these two predicted outputs, a greedy algorithm then determines the optimal location for the next laser spot movement.

In practical applications, it can be difficult to identify governing physical equations that link the desired parameters, and experimental fitting may be necessary to derive some of the model coefficients. As a solution, semi-empirical models can be employed to incorporate the physics while leveraging realistic experimental data to gain relevant insights. For example, fatigue crack growth life of AM materials can be approximated using the Paris' law by having the stress intensity tensor and some empirical material properties. Therefore, to benefit from the advantages of PIML models, Wang et al. [90] aimed at predicting the fatigue life by combining the Paris' law with ANN and SVR machine learning models. While pure physics-based models struggle due to insufficient explanatory power for the scatter of fatigue life, and pure machine learning models face issues of overfitting with limited data, the proposed PIML model demonstrated high accuracy (up to 98 % R^2) and mitigated the limitations of both pure approaches.

(iii) Data augmentation based on process physics

Data augmentation refers to increasing the size of the dataset by creating new or synthetic data points. The domain-specific physical principles may be leveraged to generate/augment new additional training data. Consequently, the diversity and quality of the training dataset may be enhanced, leading to improved model performance and generalizability.

Zhao et al. [91] developed a PIML model to obtain both forward and inverse predictions of the PBF process's process parameters and molten pool characteristics. In addition to the experimental data, a mechanistic model based on OpenFOAM software was used to augment the dataset size and train the ANN model. Moreover, the mechanistic model also exposes the fundamental causes of different prediction accuracies in the ANN model, by demonstrating the spatial and temporal fluctuations of the print tracks and molten pools. It was shown that the highest prediction accuracy of the model using both experimental and mechanistic data was 97.3 %, while it was 68.3 % when only experimental data was used. This highlights the importance of data availability, where mechanistic models act as data augmentation tools.

3.1.2. Physics-based feature engineering based on data-centric methods

As opposed to studies that use governing physical equations to perform feature engineering, physical knowledge can also be obtained using data-centric techniques. This brings in some opportunities for integrating domain expertise in PIML models. In general, the process of feature engineering consists of three main stages: 1) feature extraction, 2) dimension augmentation, and 3) feature selection. While including more input features can generally improve prediction accuracy, too many features may negatively impact the performance due to the curse of dimensionality. Conversely, getting rid of insignificant features can enhance the non-linear correlation between input features and output data, as well as speed up the learning process of the model. Thus, feature extraction, dimension augmentation, and then selecting the appropriate feature descriptor are all important factors in feature engineering of ML models. By aligning these steps with the underlying system behavior and process domain knowledge, one may identify the appropriate dimension and features that encapsulate the essential behaviors and interactions of the AM system under study. These steps can be modified independently or in combination to boost accuracy. As a result, this targeted approach can aid in feature engineering, resulting in a more compact yet informative feature space.

(i) *Feature extraction using image analysis*

Image data has proven to be a valuable source for real-time analysis and control in AM. For instance, as shown in Fig. 7., image data has the potential to reveal physics-based process signatures that can be used to predict structure-related and property-related factors in the field of AM. Smoqi et al. [94] developed a PIML model to predict porosity in PBF using meltpool signatures. First, physics-based parameters such as length and temperature distribution of meltpool as well as mean ejecta spread, and temperature were extracted from an in-situ dual-wavelength imaging pyrometer (Fig. 7 a). These parameters were used as inputs for the implementation of LOGREG, KNN, and SVM machine learning models to predict the type of porosity (lack-of-fusion, conduction, keyholing) and severity. The results of the PIML models were compared with a pure ML CNN model that had similar outputs and datasets (22,400 meltpool images) but used images as input. It was reported that the KNN PIML model with accuracy exceeding 95 % (F1-score), outperforms the other PIML and CNN models. Zhang et al. [95] developed a machine vision monitoring technique that uses high-speed imaging to extract information about the meltpool, plume, and spatter during the PBF process. As shown in Fig. 7 b, they extracted features of these components based on their signal generation mechanisms, such as the meltpool histogram features, keyhole area, plume area and intensity, plume orientation, and spatter characteristics.

Mu et al. [101] developed an online simulation model using a diffusion model to predict distortion fields. They used a vector quantized variational autoencoder and generative adversarial network for feature extraction from distortion maps and a recurrent neural network for time-scale result fusion. The model uses 2D convolutional layers for feature extraction and has an encoder-decoder structure for accurate reconstruction. Pretrained with offline finite element methods (FEM), it predicts distortion using laser-scanned point clouds during deposition, surpassing FEM by 143 % and ANN methods by 151 %. In [113], meltpool monitoring images were compressed into a compact feature vector with an encoder and reconstructed with a decoder. The goal was to break down the input meltpool images into understandable representations, providing a suitable feature space for ML models to distinguish between Non-keyhole and Keyhole pores in PBF.

Wavelet transform often helps with extracting hidden physical insights from image data and better revealing spatial and temporal information. For example, Xie et al. [96] developed a mechanistic data-driven framework to predict mechanical properties and identify dominant mechanistic features in a DED process. In their proposed framework (Fig. 7 c), the thermal histories from 135 selected regions of interest for 12 additively manufactured thin walls were converted to wavelet scalograms and used as inputs of the CNN model to predict the ultimate tensile strength, yield strength, and elongation. The model is trained using the data obtained from the miniature tensile specimens at the regions of interest. Then, the trained model was utilized for the prediction of mechanical properties throughout the printed walls, having IR thermographic data without any need for additional tensile specimens. It was observed that the proposed approach reaches an R^2 score of 0.7 using only a small amount of noisy experimental data, while traditional methods have an R^2 score of 0.2-0.6.

Faegh and Haghighi [104] proposed a conditional generative adversarial network to generate the PBF temporal thermal data with process domain knowledge fused into the image generation procedure. Laser power, scan speed, laser spot size and time step were utilized to generate images. It was indicated that the model was able to generate synthetic sequential thermal images close to the experimental data at various combinations of process parameters. Chen and Guo [105] developed a deep learning framework by incorporating physical constraints to predict porosity in laser metal deposition processes. Their

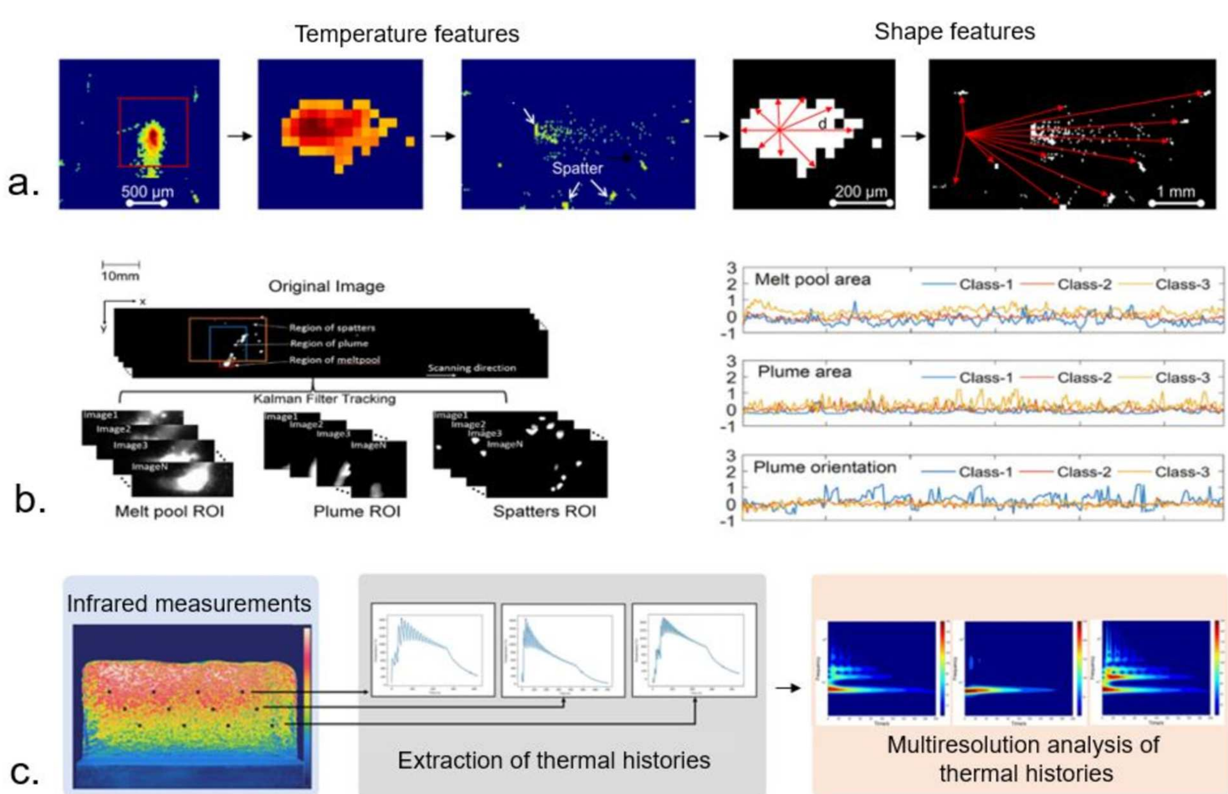

Fig. 7. Feature engineering based on image data using a. shape feature extraction [94], b. meltpool histogram features [95], c. wavelet transform [96].

approach utilizes a deep convolutional generative adversarial network for generating data, which is further refined by a Kullback-Leibler divergence-based model that captures the melt pool's shape and temperature distribution. To ensure the generated data aligns with physical properties, a control chart is employed. A convolutional neural network is then used to predict porosity labels. Their model demonstrated superior predictive performance compared to traditional deep learning benchmarks.

(ii) *Feature extraction using multi-stage machine learning*

Machine learning models as promising data-centric techniques can be used in multiple stages to extract and utilize physically important intermediate/transient features that are difficult to obtain via governing physical equations. Gaikwad et al. [97] extracted physics-based features of meltpool from a pyrometer and high-speed video signatures in the PBF process via a sequential decision analysis neural network (Fig. 8). First, the statistical probability distribution features extracted from the pyrometer are used in the first echelon ANN to predict the laser power and velocity. Then, meltpool features derived from the high-speed video camera were utilized to predict the mean width and standard deviation in the second echelon ANN and single-track continuity in third echelon ANNs. It was concluded that the proposed model outperforms the pure data-driven models both in terms of accuracy and computational time.

Ren et al. [98] developed a PIML model to predict the meltpool size in a PBF process using a two-level ML approach. First, process parameters and the laser position were used as the inputs of the lower-level ML model to predict a pre-scan initial temperature. The predicted temperature was considered as a physics-based parameter that depends on the thermal history of the meltpool. It was then employed as input for the upper-level ML model to estimate the size of the meltpool. The ML models used at the upper level were comprised of GPR, ANN, regression-based, and tree-based models. The results showed that the PIML model's prediction accuracy was significantly better than that of the ML model, lacking a physics-based initial temperature input.

By using transfer learning, multi-stage machine learning models can lead to more generalized and well-performing PIML models even with a limited dataset [112]. In this approach, target data from the source process model increased in steps to iteratively identify the smallest amount of experimental data needed for transfer learning. The goal was to get a final error on unseen experimental data that is less than or equal to the error from directly using the experimental data. The reduction in experimental costs was around 60 %, and computation time was at least 10 times lower with their proposed Smart ML. Wenzel et al. [99] developed a PIML method that optimizes reliability by suggesting optimal print parameters in the MEX process. First, an RNN was used to conduct knowledge transfer by generating the behavioral vector using input/output observations obtained from a particular 3D printer. Then, an ANN was utilized to generate an estimation of the target values considering various sets of inputs and the obtained behavioral vectors for a specific printer. If the conditions change, the behavior of the 3D printer changes as well, and the behavioral vector can be updated by the RNN accordingly. Moreover, an ANN encoder-decoder is used to define the behavioral vectors for various known systems. The encoder-decoder is trained using predictions from a Latin hypercube sampling design of experiment method. This real-time knowledge transfer eliminates the need for retraining and enhances the reliability of 3D printing by enabling real-time response to changing conditions. The method proposed in this study achieves a lower RMSE in predicting unknown experiments with limited measurements compared to statistical approaches, thanks to the application of transfer learning from domain knowledge.

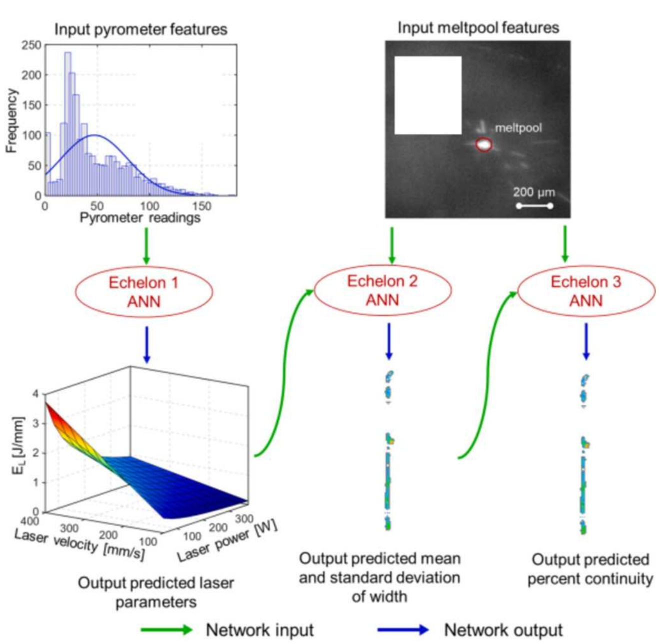

Fig. 8. Feature engineering based on multi-stage machine learning [97].

(iii) *Dimension augmentation by incorporating feature interaction terms*

For an ML model to provide accurate and reliable predictions, the input features must be of high quality, representative of the problem domain, and properly preprocessed. A promising way to do this is to increase the number of features by incorporating feature interaction terms that can be considered as a high-dimensional set of parameters built on nonlinear combinations of the main features.

As an example, Wang et al. [100] predicted the quality of CoCrFeNiMn high-entropy alloys built via PBF. The inputs of the model are comprised of physics-informed features such as peak temperature of the molten pool (T_{max}) and Marangoni flow (*Ma*) as well as process parameters such as laser power (*P*), scan speed (*v*), hatch space (*h*), and layer thickness (*t*), as shown in Fig. 9a. Also, a dimension augmentation procedure was used to expand the process parameters (laser power, hatching space, scanning speed, and layer thickness) into an optimal high-dimensional set of process parameters as shown in Fig. 9b. The original 4-dimensional features are combined through nonlinear combinations in the forms of x, $x^{1/2}$, x^2, x^3, and log (1 + x) to provide a 206-dimensional feature space. These high-dimensional features were used as inputs of the ML model, and their significance is determined using the RF algorithm, with the resulting mean squared errors being recorded. Ultimately, 40 optimal features with minimum mean square error were used as the final model inputs. The introduced model was utilized to predict the top layer surface roughness (*Ra*) and relative density (ρ). The dataset was used to train ANN, SVM, and RF machine learning models, and it was concluded that the SVM has better generalization capability and prediction accuracy. Moreover, the utilization of both dimensionally augmented features and physics-based input led to better results compared to the pure ML model trained with original process parameters.

(iv) *Dimension augmentation by deriving feature statistics*

Inclusion of several features as inputs, especially in the cases where parameters are in the form of time-varying signals, increases the number of variables and might result in overfitting. A promising way to tackle this is to incorporate statistical measures of the existing features. Based on the physics of the problem, the statistical measures might be considered as potential physical indicators of the problem. For instance, maximum temperatures in metal AM are a determinant of the subsurface porosity [117], and statistical measures such as skewness and kurtosis can be used to represent time-varying signals and the time spent at

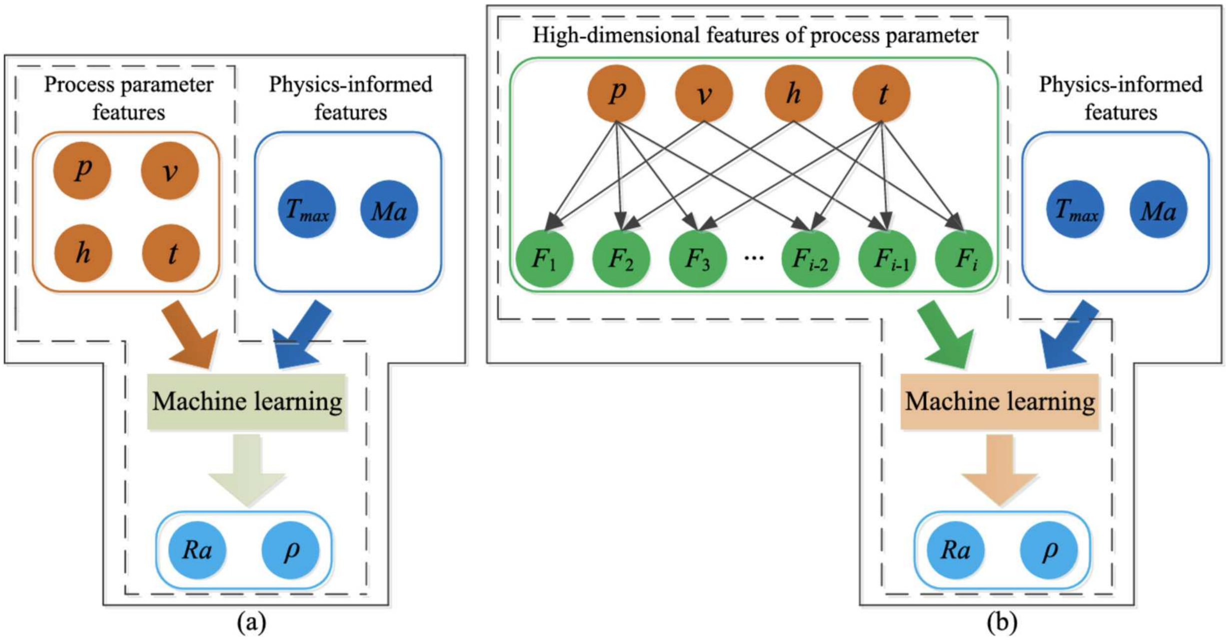

Fig. 9. Feature engineering by dimension augmentation [100].

extreme values.

Following this approach, Cooper et al. [106] proposed a PIML model to predict the ultimate tensile stress and yield stress in DED-fabricated parts. In addition to the temperature values, they utilized the first and second partial derivatives of temperature during DED as they can represent grain size and local material density, respectively. As these features were time-varying signals, statistical measures like maximum, mean, variance, skewness, and kurtosis of them were used as model inputs. Moreover, Lei et al. [102] combined process parameters such as laser power, laser speed, energy density, scanning phase, and sequential information such as layer number and section order with the statistical features of each layer. It was shown that the inclusion of physics-based features improves the model's explainability and performance.

(v) *Feature selection by leveraging features significance on the output*

As mentioned previously, feature extraction and dimension augmentation are usually followed by a feature selection method to reach the desired performance criteria of the PIML model. Various feature selection methods are adopted by researchers based on the datasets, the problem, and the algorithm being used. As the extracted features might have some redundant information, principal component analysis (PCA) can be used as a feature selection scheme to identify the most important features. For example, Zhang et al. [95] utilized the SVM-PCA classification method to assess the quality level, i.e., track width, using different combinations of features in the PIML modeling of the PBF process.

In another study, Xie et al. [96] aimed to identify dominant mechanistic features in a PIML model of the DED process by defining a parameter based on the occurrence of temperature data within discrete ranges of thermal histories. The relationship between this parameter and tensile strength is studied using an RF algorithm to detect the most important temperature ranges. The identified important ranges are related to physics-based properties such as material phase transition temperatures and measured dendritic arm spacing. The proposed model was compared with ten ML models, which are a combination of different dimension reduction techniques (Discrete binning, PCA) and regression methods (ANN, KNN, Tree-based models, etc.). It was concluded that the proposed model with wavelet transform as its feature engineering method and CNN as the ML part outperforms the other investigated models.

Historically, bidirectional stepwise regression methods have been employed to select features in predictive models, with the constraint that only one feature is included or excluded at a time. Stepwise techniques tend to be less efficient and may overlook the overall best combination of features. To address this concern, one approach is to utilize Shapley additive explanation (SHAP) based feature engineering. For instance, SHAP values were calculated using the metric of cumulative relative variance in [106] to measure the impact of each input feature on PIML modeling of tensile property of DED parts. Then, using an additive utility function, an optimal subset of the features that minimize the loss function was identified. It was concluded that the proposed model has six orders of magnitude fewer parameters than previous models in the literature, while achieving similar or higher predictive accuracy. Moreover, utilizing SHAP values to evaluate the contribution of metal AM process parameters on the microstructure evolution has shown promise in forming more explainable artificial intelligence-based models [107]. Furthermore, melt pool depth was calculated using SHAP analysis of atomic features in [108].

3.1.3. *Physics-based feature engineering based on both governing physical equations and data-centric methods*

(i) *Dimension Augmentation*

Feature engineering for PIML models using data obtained from mechanistic models and process data (e.g. images, sensor data, etc.) separately has been discussed so far. A potential approach in feature engineering of PIML models is to combine image data with data obtained from mechanistic models to leverage hybrid sources of physical knowledge. Guo et al. [109] developed physics-driven deep learning models for predicting the pore occurrence and its size in a DED process as depicted in Fig. 10. First, a pure CNN model, called PyroNet is developed to map pyrometer data to porosity by learning hidden patterns and structures in thermal images of meltpool. Next, a physics-based model, named PyroNet+, is developed which has the number of layers as an additional input compared to PyroNet. To incorporate more physical features, another physics-driven model named PyroNet++ is developed in which the length, width, depth, and temperature of meltpool gathered from FEM simulations are considered as additional inputs

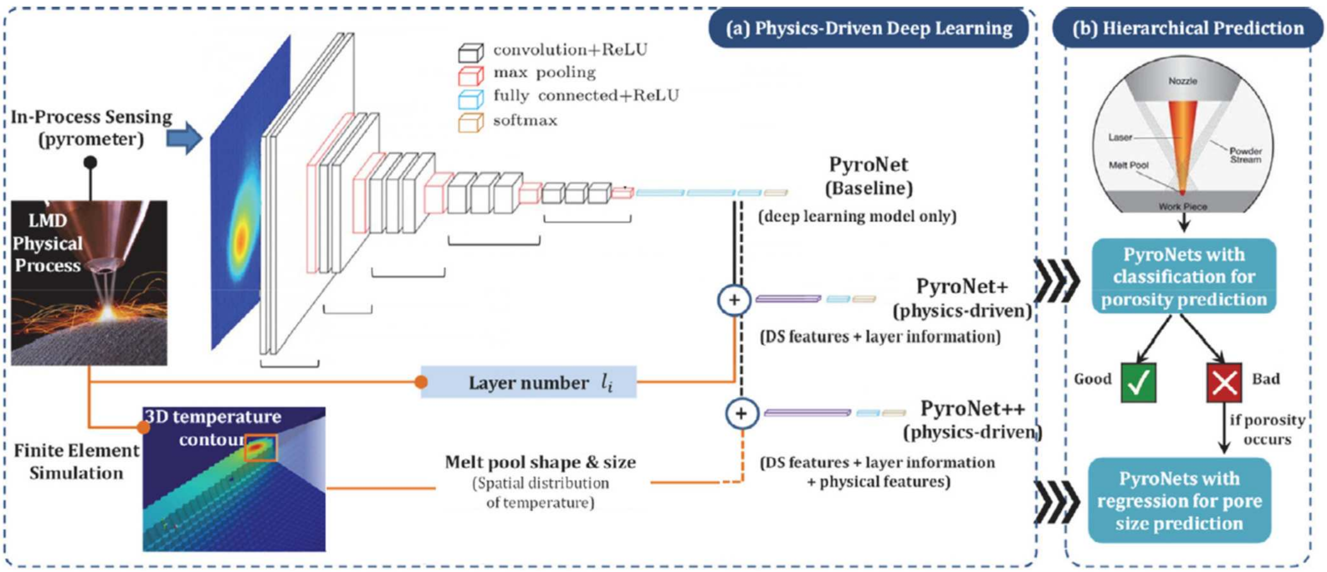

Fig. 10. Feature engineering based on both governing physical equations and data-centric techniques [109].

compared to PyroNet+. It was shown that the physics-driven PyroNet++ model outperforms the PyroNet and PyroNet+ models in predicting the pore occurrence. Moreover, the severity of porosity is predicted using the three developed models. Mean absolute percentage errors of 8.99 %, 8.91 %, and 6.91 % are reported for PyroNet, PyroNet+, and PyroNet++, respectively.

Wang et al. [114], employed data-centric techniques to enhance prediction accuracy and generalizability by removing highly correlated and normalizing features in LPBF process. Moreover, additional features from a continuous damage mechanics model was utilized. It was reported that the proposed PIML method outperforms the black-box model that uses raw features from experimental conditions, mechanical properties, porosity analysis, and surface morphology.

To capture the variety of shapes that meltpool boundaries can take in a DED process, Gawade et al. [110] used Functional PCA as a feature engineering technique, while FEM simulation was used to analyze the thermal gradients and cooling rates of the meltpools. Functional PCA, in contrast to PCA, resolves functional data into component representations that accurately analyze the variability of the structure of meltpools. By doing this, they were able to reduce the amount of required computational cost. Their proposed approach, which uses a Gradient Boosting method, performed well on both the training and testing datasets for Ti-6Al-4 V thin-wall structures. Zamiela et al. [115] integrated infrared thermal data obtained during Wire Arc DED with the Goldak double-ellipsoidal heat flux model to simulate the process energy input. Next, they developed a physics-based input to represent the internal thermal history. Finally, a CNN was employed to map the relationship between the three-dimensional thermal gradients and the resulting surface deformations.

(ii) *Data Augmentation*

A promising way to develop PIML models is to combine real-time extracted data with multiple physical models. To do so, Oikonomou et al. [111] proposed a PIML model that combines jet features extracted in real-time by a machine vision plus a machine learning module and the same features obtained from a physics-based modeling module. They developed a physics-informed learning framework for electrohydrodynamic polymer jet printing with two GPR models and two physical models. The jet radius profile and the jet lag distance were extracted from machine vision as well as physical models to represent the printing process dynamics. In the machine vision module, image analysis, along with the first GPR model (high-fidelity), outputs these features. The jet multi-physics model and geometrical model are the two physical models to extract the same features. Later, the data from both these modules are combined and used as inputs for the second GPR (multi-fidelity) model. To explain more, multi-fidelity was used to approximate the relation of jet radius and lag distance with nozzle tip to collector distance and collector to jet speed, respectively. The proposed framework has a variety of distinctive capabilities that include real-time extraction of features through computer vision and the use of physics-based capabilities, which aim to minimize the experimental cost while maintaining accuracy and robustness. Similarly, PIML models can be developed by utilizing statistical techniques when combining data from physical models and experiments. For example, Li et al. [116] built the PIML model training dataset first by creating a probabilistic model from experimental data and later combining it with thermal-fluid simulation data of melt pool depth and width by using kullback-leibler divergence method.

3.2. *Physics-based architecture shaping for PIML models*

In addition to feature engineering methods discussed in the previous section, physical knowledge can be fused into the architecture of the ML models themselves. In this section, different approaches for the architecture shaping of PIML models in the field of AM are discussed based on the methodology used for shaping the architecture. It is worth noting that any change in the machine learning model, i.e., the way the links or nodes are connected, or weights, biases, and activation/kernel functions are defined, based on physics, is considered as an architecture shaping the PIML model in the current review paper. As shown in Fig. 11, the methodologies used for physics-based architecture shaping in PIML modeling of AM processes can be categorized into deep unfolding methodology, graph-based approaches, and RNN-based networks. An overview of the physics-based architecture shaping models for PSP modeling in AM processes, as well as the sources of physical knowledge and integration details, are discussed in this section, and a summary is reported in Table 4.

3.2.1. *Architecture shaping using deep unfolding methodology*

Deep unfolding, also referred to as model-based deep learning or algorithm unrolling, represents one of the emerging AI-driven approaches suitable for situations where data is limited, but an existing iterative model is present, offering potential advantages to the training

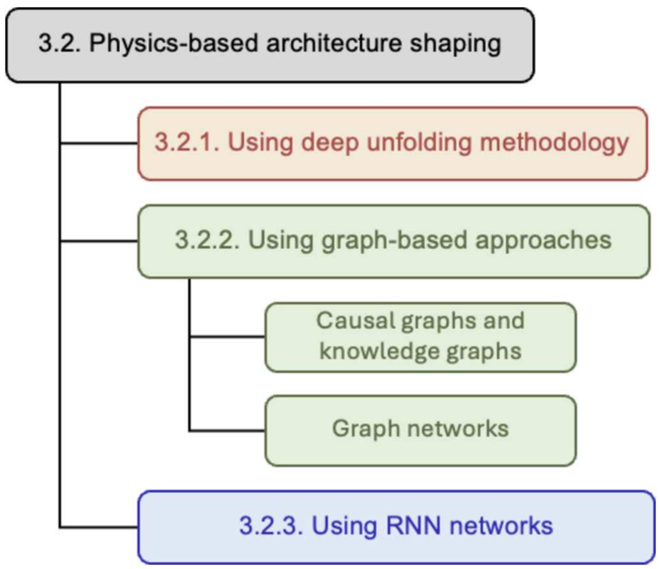

Fig. 11. Categorization of the reviewed PIML methods based on physics-based architecture shaping.

of ML models [126,127]. Inspired by the deep unfolding concept, Ghungrad et al. [118–120] introduced a method for physics-informed architecture shaping of ANNs towards AM process signature modeling. The proposed architecture-driven physics-informed deep learning structure, uses a deep unfolding approach to predict thermal history in the PBF process (Fig. 12 a). The model is based on iterative thermal model equations, and each iteration of the transient thermal model corresponds to a layer in the neural network structure, as shown in Fig. 12 b. In each layer, both the temperature data from the previous iteration and the inputs are processed to calculate the temperature in the current iteration. Unlike traditional neural networks, the weights and biases in architecture-driven PIDL are linked to the equations of the transient thermal model and play the role of coupling physical knowledge into the model architecture. Unfolding the transient thermal equation iterations into the layers of neural networks and defining the weights and biases based on governing physics makes APIDL more interpretable compared to a black-box ANN, where connections are established solely through data. The models are trained and tested using a limited experimental dataset with the TensorFlow library in Python. The architecture-driven PIDL model was compared with other algorithms such as ANN, extra trees regressor (ETR), LSTM, and SVR. It was shown that for limited data scenarios, the proposed APIDL structure outperforms the other models with a testing mean absolute percentage error of 2.8 % and an R^2 value of 0.936. This highlights the importance of physics fusion in ML models that reduce the data requirements.

3.2.2. Architecture shaping using graph-based approaches

Graph-based approaches are gaining attention in recent years as they enhance the interpretability and generalizability of ML models. These approaches utilize graph structures to represent and analyze data. The architectures of graph-based approaches vary, but they all encompass common elements, i.e., entities (elements with attributes), relations between entities, and a rule that maps entities and relations to other entities and relations [128]. Based on the application domain and specific functionality, various graph-based approaches, such as knowledge graphs, causal graphs, and GNN, have been developed.

- Causal graphs and knowledge graphs

Causal graphs are graphs that have cause-and-effect relationships to understand the causal mechanisms [129]. As causal mechanisms are much easier to explain and interpret, integrating them with ML models would enhance the interpretability. Nagarajan et al. [121] developed a knowledge-based topology design for ANN by integrating the pure ANN model with dimensional analysis conceptual modeling (DACM). The knowledge that has been encoded is expressed through causal graphs, as shown in Fig. 13. These graphs, which are created using DACM, are utilized to define the structure of ANNs, where variables can be seen as neurons, and the graph resembles an ANN. There are two kinds of weights in this model: the first type is already obtained based on prior knowledge (physical equations) and requires no further training, while the second type has unknown weights that must be calculated through training with data. Therefore, experimental/simulation training data is only necessary for the zones where prior knowledge is lacking or

Table 4
Summary of studies on physics-informed architectures based on a. governing physical equations, b. data-centric extraction, c. both physical equations and data-centric extraction.

Ref	Year	AM process	ML method	Integrated physical knowledge	Dataset size	Target
a. Source of physical knowledge based on governing physical equations						
[118]	2021	PBF	ANN	Transient thermal model	300	Temperature
[119]	2022	PBF	ANN	Transient thermal model	500	Temperature
[120]	2023	PBF	ANN	Transient thermal model	1000	Temperature
[121]	2019	MEX	ANN	DACM framework and CFD simulations	100	Wall thickness, height, and mass of a part
[122]	2022	MEX	RNN	Physics-based weights and activation functions	252	Height evolution
[123]	2022	PBF	GNN	Simulating microstructure evolution using the phase-field method	–	Temperature field, liquid/solid phase fraction, and grain orientation variables
b. Source of physical knowledge based on data-centric extraction						
[124]	2020	MEX	LSTM	Weight calculation using the sequence of thermal states, material properties, and machine settings	144 experiments	Part tensile strength prediction
c. Source of physical knowledge based on both governing physical equations and data-centric extraction						
[53]	2022	PBF	ANN	Knowledge graphs	4700, 118,928 images	Capture dynamic characteristics of PSP relationships
[125]	2021	DED	GNN, RGNN	Nodal and element features	55 geometries	Thermal histories

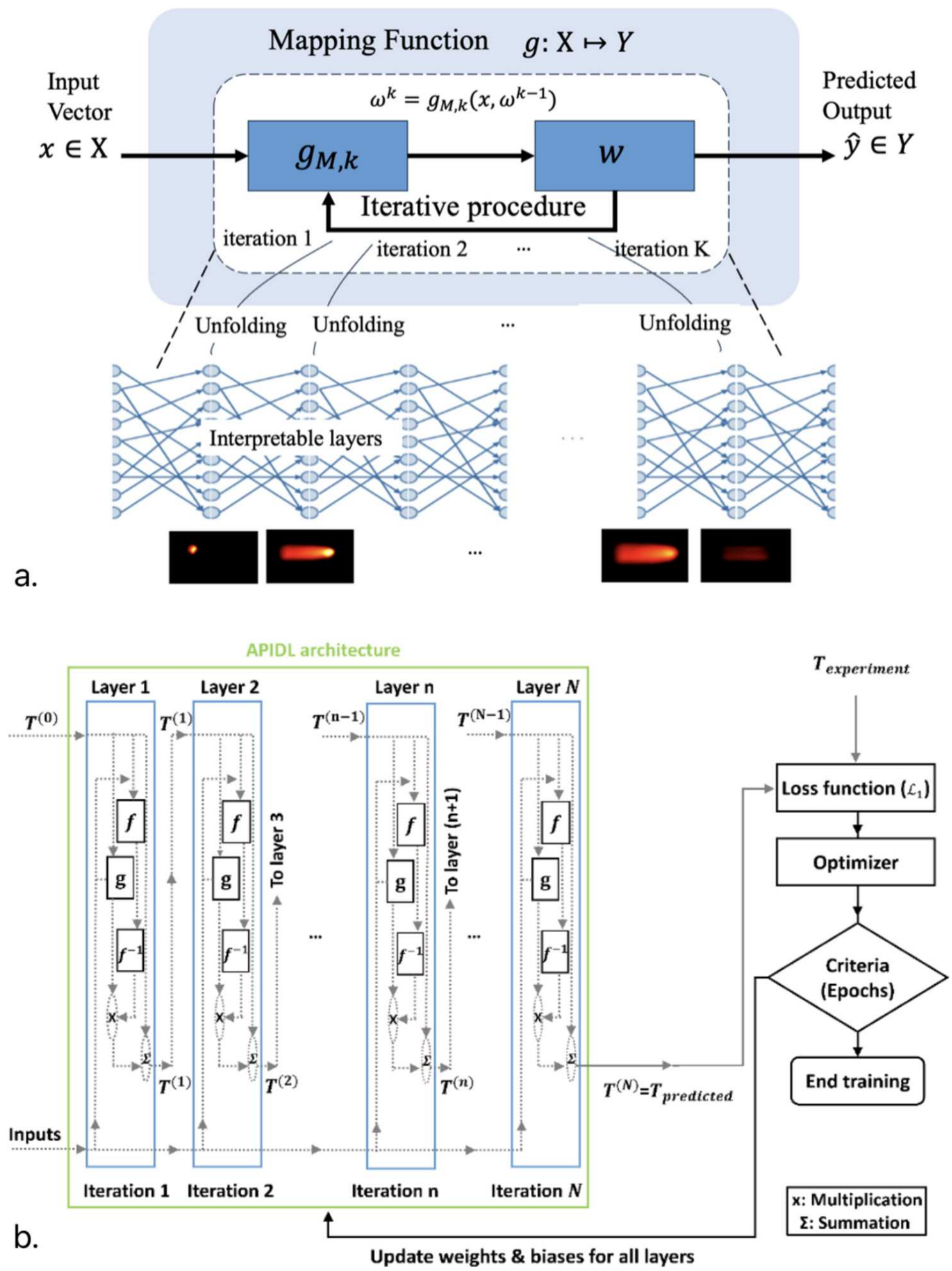

Fig. 12. Architecture shaping of PIML model using deep unfolding, a. overview, b. train procedure [120].

difficult to acquire. A case study was done to model wall thickness, part height, and total part mass in an MEX component using four ANNs following a causal graph. It was shown that the knowledge-based ANN model, which required fewer training weights due to the use of physical knowledge, exhibited more robust generalization than a pure ANN model.

In addition to the simple cause-and-effect relations (i.e., causal graphs), knowledge graphs containing pre-existing information about physics with ML models [130] can be used to create more comprehensive relationships. To convert unstructured AM data obtained from measurement and monitoring into structured descriptive data with relevant PSP features, Ko et al. [53] proposed a knowledge graph integrated PIML framework. This framework was utilized to create predictive PIML models and establish relationships between data. The framework consists of three tiers, including knowledge of predictive PSP models and physics, PSP features of interest, and raw AM data. The feature extraction process was guided by the physical insights derived from the knowledge graphs in the knowledge tier. Then, PSP features were extracted from raw data, fused, and ultimately utilized as inputs for predictive PSP machine learning models. A continuous learning scheme is utilized to iteratively update the PSP models via ML models and then deploy these models to monitor and control real-time decisions. An advantage of this scheme is that it supports the continuous addition of data in the AM database and the modification of predictive ML models and PSP knowledge.

- Graph networks

Graph networks are models designed to work with data represented in graph structures to learn and make predictions. Xue et al. [123] considered the dynamic microstructure evolution in AM as an ML task similar to the message-passing procedure of a graph network. They formulated the discretization of a phase field method, a physics-based computational method for simulating interfacial morphology, as an

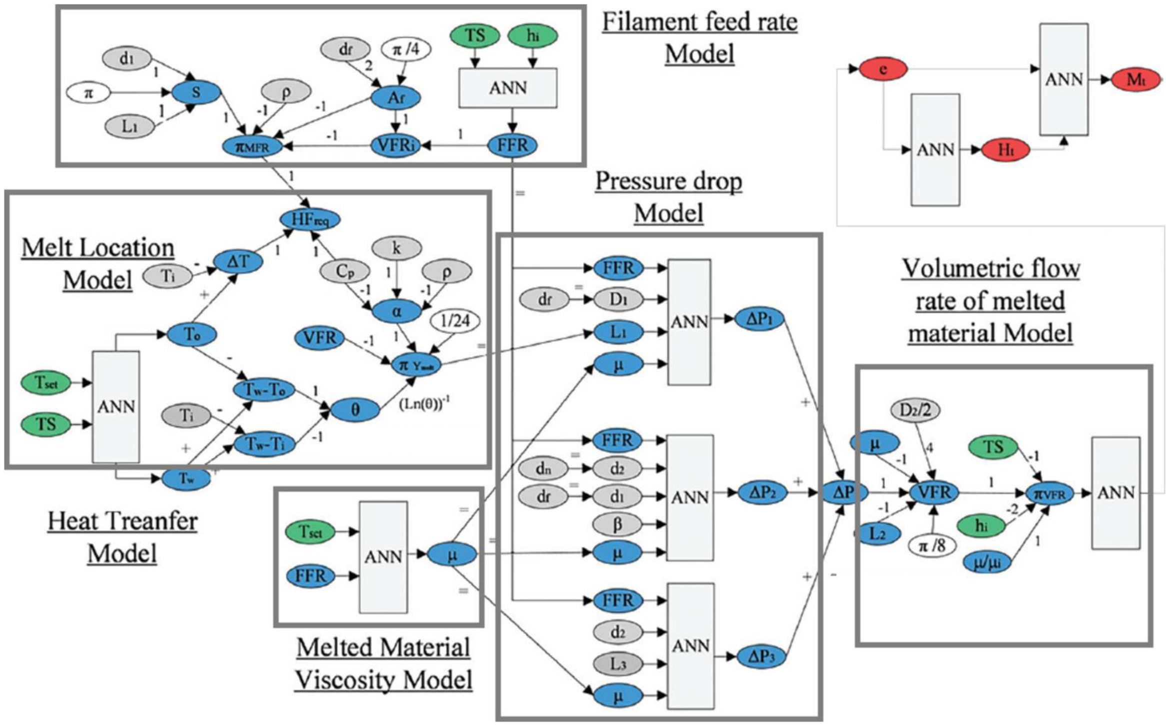

Fig. 13. PIML model architecture shaping using causal graphs [121].

ML problem on a graph. In contrast to the loss function definition in ML, they minimized a physics-based free energy formula, as shown in Fig. 14. Results showed that the proposed approach can detect effective physical features and is at least 50 times faster than direct numerical simulations.

The GNN is a subset of graph networks where the rules are neural network functions [128]. To benefit from the capabilities of GNN, Mozaffar et al. [125] proposed two GNN architectures to capture the spatiotemporal dependencies of thermal responses in AM processes. They suggested that these dependencies, which are typically modeled

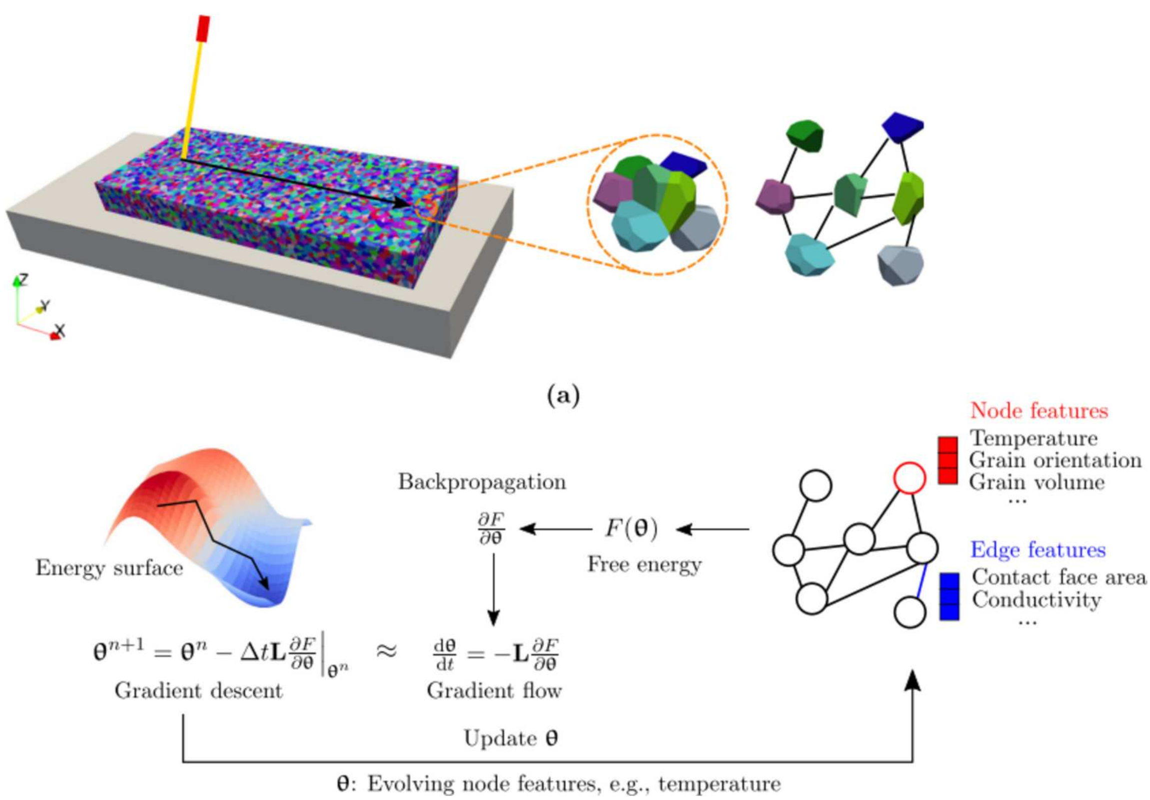

Fig. 14. Physics-informed graph network for a single-layer, single-track PBF process [123].

using physics-based simulations like FEM, can be alternatively modeled using GNNs. Their hypothesis is based on the similarities between the assembly operations of finite element matrices and message-passing formulations in GNNs. As shown in Fig. 15, the first GNN architecture predicts a single-time step update in each training instance, while the second GNN architecture, called Recurrent Graph Neural Network (RGNN), generates time-series thermal responses over multiple time steps. The models were trained and tested on 55 industrial-grade geometries, varying in size, layers, shapes, and geometric features and meshed using ABAQUS to 8-node hexahedron elements. The database was created using graph representations where each node of the mesh was defined as a node in the graph, and edges were defined based on the connectivity matrix indicating common elements. Linking the similarities between the assembly operations of finite element matrices and message-passing formulations in GNNs makes GNNs more interpretable. The results showed that both GNN and RGNN models had good agreement with the ground truth, with RGNN outperforming GNN in capturing long interactions. However, RGNN required five times more epochs compared to GNN. Overall, it was concluded that the GNN architectures provide a practical substitute for conventional computational approaches.

3.2.3. Architecture shaping using RNN networks

Employing recurrent neural networks (RNNs) can aid in uncovering the relationship between the fundamental mechanisms in the AM process and the resulting quality of the fabricated component. To benefit from this capability of RNNs, Zhang et al. [124] added an attention mechanism to an LSTM network for predictive modeling of MEX parts quality. They created an encoder-decoder structure to connect the thermal states of each layer to the properties of the printed object. The encoder consisted of a two-layer LSTM network, with each print layer represented by one LSTM cell, as illustrated in Fig. 16. The decoder predicted the tensile strength of the part based on a weighted sum of all the thermal states from the last LSTM layer in the encoder. These weights represented the influence of each layer on the part property, but they were traditionally kept constant after network training, which could be problematic for modeling dynamic relationships. To address this issue, the authors introduced an attention mechanism that determined the weights using the sequence of thermal states, material properties, and machine settings, such as extruder temperature, printing speed, and layer height. The addition of the attention mechanism reduced prediction errors in tensile strength by 30 % compared to a standard LSTM.

In another application, Inyang-Udoh and Mishra [122] developed a PIML model for the height evolution of parts printed in droplet-based

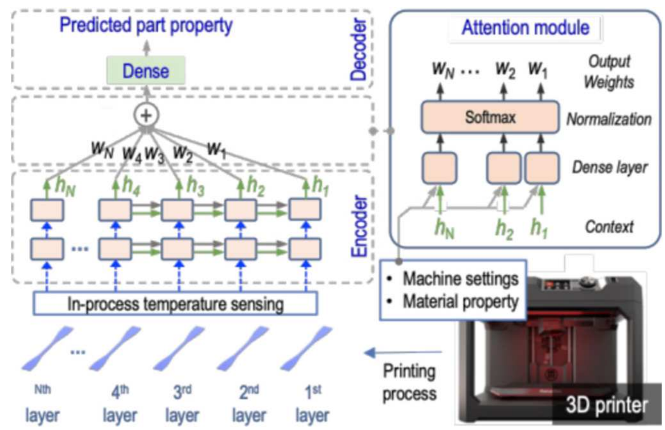

Fig. 16. Attention-based encoder-decoder for part property prediction [124].

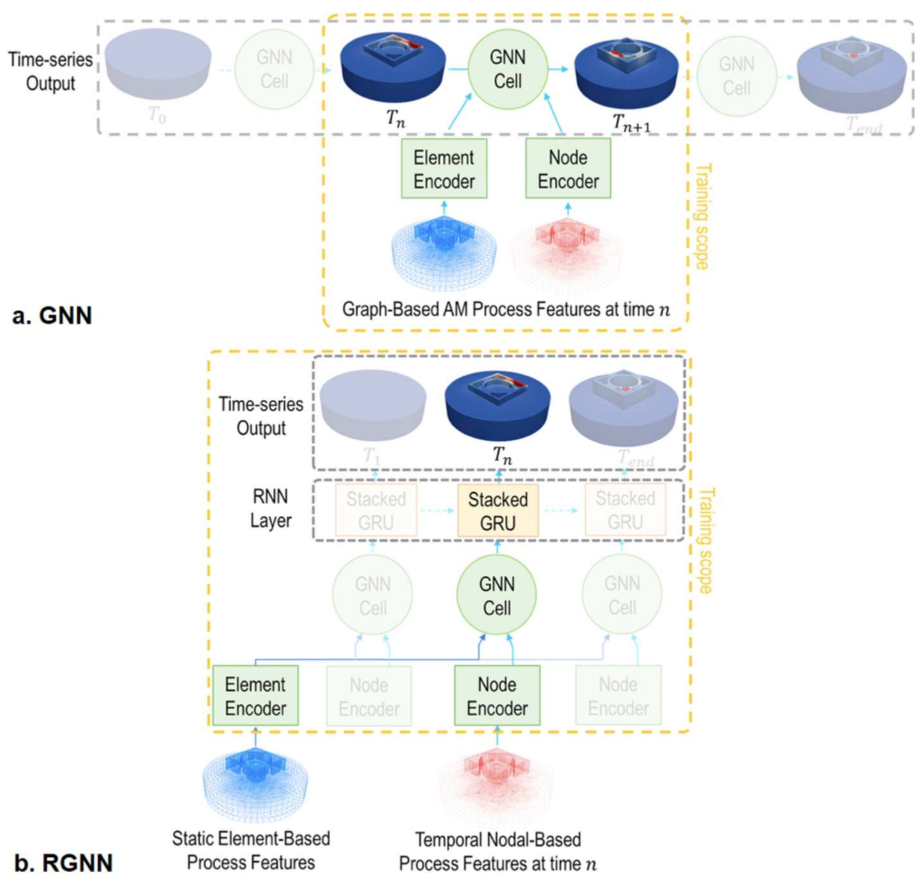

Fig. 15. Network block diagrams and training details for a. GNN, b. RGNN models [125].

AM. The model is a convolutional RNN, and its architecture considers mass conservation during the height evolution. They incorporated physics into the architecture by adjusting the weights as well as activation functions. It was concluded that the developed model has 1.7 times smaller test RMSE when trained with only two orders of magnitude less data compared to a black-box ANN model.

3.3. Physics-based loss function modifications for PIML models

Integration of physics in ML modeling of AM processes by feature engineering and architecture shaping was discussed in previous sections. In addition to these two fusion approaches, fusion of physical knowledge during the ML model training, evaluation, and tuning may be considered as a third class of PIML models. Specifically, as the data feeds into the ML model, it passes through a loss function to calculate the errors and update the model parameters to reach the desired accuracy. Consequently, incorporating physical knowledge into the loss function has been frequently studied in the literature. A review of physics-based loss function modification approaches to building PIML models for PSP modeling in AM processes is discussed in this section. Similar to the physics-based feature engineering and architecture shaping, the source of physical knowledge fused in loss function can be based on both governing physical equations and/or extracted from data using data-centric techniques. As shown in Fig. 17, the studies in this section are categorized into two main groups: (1) those that perform loss function modification through encoding residuals of physical differential equations in the loss function and (2) those that perform loss function modification through incorporating physics-based parameters in the loss function. In each category, the details on the source of physical knowledge and integration details in the loss function are discussed in detail, and a summary is reported in Table 5.

3.3.1. Encoding residuals of physical differential equations in the loss function

Recently, the integration of physical differential equations into neural networks' loss function to create PIML models, often called PINNs, has been frequently studied. For example, the governing fluid-flow equations in the AM process can be coupled with neural networks to form a PIML model. The fundamental concept behind this category of PIML involves utilizing a neural network to estimate the solution to PDEs or ordinary differential equations. This neural network is trained through the minimization of a loss function that is determined by the difference between the residuals of the PDEs and corresponding boundary and initial conditions. The automatic differentiation capability of ML packages (in PyTorch and Tensorflow, for example) is a powerful tool to calculate the required gradients in governing PDEs and their initial/boundary conditions [152].

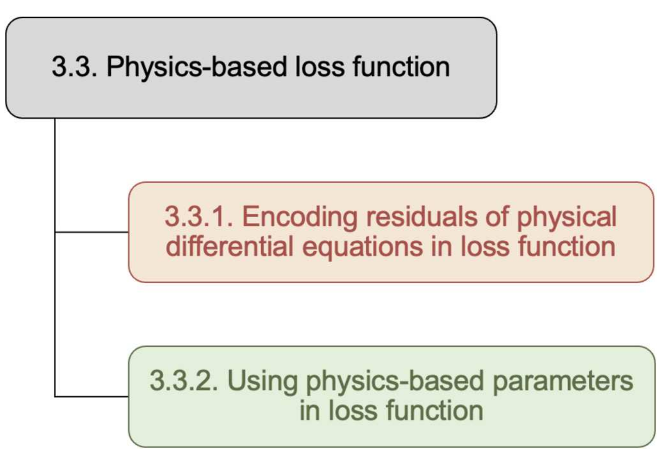

Fig. 17. Categorization of the reviewed PIML methods based on physics-based loss function.

Governing physical equations for different AM technologies can be solved using the modified loss functions technique. Liao et al. [132] developed a PIML model for the DED process to predict the full-field thermal history and unknown material/process parameters using partially observed temperature data as input. As shown in Fig. 18, they defined a loss function that combines the residuals of the PDEs, the boundary conditions, and the initial conditions, along with an additional data-based loss term that uses experimental or simulated temperature data as the ground truth. The PIML model was able to predict both simulated and experimental temperatures with RMSE of 14.07 K and 47.28 K, respectively. It was reported that the inclusion of an auxiliary data term in the loss function led to the same level of accuracy in only one-third of the epochs required without this additional term. They also found that a pre-trained model required less than one-fifth of the number of epochs compared to a randomly initialized model to reach the same level of accuracy. By using this approach, the PIML model predicted the laser absorptivity, heat capacity, and thermal conductivity with errors of less than 5 % compared to corresponding simulated values. Using a similar methodology to fuse governing equations into the loss function, the study of gas flow meltpool in PBF, as well as temperature distribution during the cooling phase in the VPP process are reported in [133,135], respectively. It was concluded that the PIML models require only a limited dataset [133,134] and are more suitable for industrial applications [135].

In physics-based loss function modification of PIML models, various terms related to governing PDEs, and data terms are integrated into the loss function. Fusion of different terms in loss functions is usually done by using a weighted sum approach. Li et al. [136] predicted the 3D temperature field during the deposition and cooling stages of the DED process using a PIML model. The weights of loss terms were considered as one for PDE and initial condition residuals and 10 for boundary condition residuals. The predicted temperature fields from this approach were in good agreement with FEM results, with a maximum relative error of about 2 % for the entire process, and an absolute error of less than 10 K at the end of the cooling stage.

As fusion of physical terms in loss functions by weighted summation might have an impact on the learning process, Zhu et al. [139] proposed a hard-type approach for Dirichlet boundary conditions based on a Heaviside function and combined it with PDE loss term. This hard-type approach can not only precisely satisfy the Dirichlet boundary condition but also speed up the learning process, compared with the conventional soft approach that uses additional constraints in the loss function to enforce the boundary condition. The investigations demonstrated that the PIML approach can accurately predict temperature and meltpool dynamics during metal AM processes, without requiring large amounts of data.

In addition to adjusting the summation methodology of different terms in the loss function, it is also important to tune the hyperparameters of the model to reach the desired accuracy. Usually, trial and error methods are used for finding the best set of hyperparameters. However, more advanced tools, such as grid search methods, can also be implemented to obtain the best set of hyperparameters and eventually better trained models. Xie et al. [140] utilized a grid search method to find the optimal combination of hyperparameters for a PIML model developed to predict the 3D temperature distribution in both single-layer and multi-layer DED processes. The PIML model was trained with a loss function that combined data, heat conduction PDE, initial, and boundary conditions, and it was reported that the model had an error rate of 2.61 %. In contrast, models that included only data or PDE terms in their loss function had higher error rates of 7.52 % and 82.6 %, respectively. They compared the performance of the PIML model with pure ML models such as ANN, LSTM, and XGBoost, and found that the PIML model had additional extrapolation ability and accurately predicted temperatures with a mean relative error of 4.83 %. It is worth mentioning that the training time for the PIML model was longer than

Table 5
Summary of studies on physics-informed loss functions based on a. governing physical equations, b. physical equations and data-centric extraction.

Ref	Year	AM process	Integrated physical knowledge	Dataset size	Target
a. Source of physical knowledge based on governing physical equations					
[132]	2023	DED	Data term and transient heat conduction PDE with corresponding initial and boundary conditions	100,000 labelled data points	Temperature prediction and parameter identification
[133]	2023	PBF	Data term, PDE residual, and boundary condition fitting	10,000 data points	Temperature and velocity field
[134]	2023	DED	Data term and transient heat conduction PDE with corresponding initial and boundary conditions		Temperature and meltpool dimensions
[135]	2021	VPP	Values and partial derivatives of temperatures	200,000 data points	Predicting thermal behavior
[136]	2023	DED	Transient heat conduction PDE with corresponding initial and boundary conditions	10,000,000 temperature outputs	3D temperature field
[137]	2024	PBF	Transient heat conduction PDE with corresponding initial and boundary conditions		Temperature and meltpool size
[138]	2024	PBF	Transient heat conduction PDE with corresponding boundary conditions		Temperature
[139]	2021	PBF	Residuals of conservation equations of energy, mass, and momentum	788,651 points	Temperature and meltpool dynamics
[140]	2022	DED	Data term and transient heat conduction PDE with corresponding initial and boundary conditions	7000	3D temperature field
[141]	2022	PBF	Transient heat conduction PDE with corresponding initial and boundary conditions	524,288 points	Temperature profiles and meltpool dimensions
[142]	2023	PBF	Transient heat conduction PDE with corresponding initial and boundary conditions	524,288	Temperature and meltpool dimensions
[143]	2021	PBF	Transient thermal model with corresponding conduction, convection, and heat generation	5000	Temperature history throughout a solid object
[144]	2023	PBF	Conduction and convection finite difference equations	5000	Temperature
[145]	2020	MEX	Displacement-based equations	39 experiments	Bond quality and porosity
[146]	2024	PBF	Physical law related to the fatigue life		Fatigue life
[147]	2022	DED	Various combination of physical variables such as maximum melt pool temperature, melt pool length and width in loss function	–	Porosity
[148]	2024	PBF	Data term and transient heat conduction PDE with corresponding boundary conditions	–	Temperature
[149]	2024	PBF	Data term, energy and Navier-stokes PDEs with corresponding initial and boundary conditions	50-13,500 points	Temperature, velocity, pressure
b. Source of physical knowledge based on both governing physical equations and data-centric extraction					
[150]	2023	PBF	The Murakami formulation indicates the relation between the fatigue limit and the characteristic defect size	561	Effect of process parameters on the fatigue response
[151]	2022	PBF	Semi-empirical modeling approach to fatigue life based on linear elastic fracture mechanics	12 samples	Fatigue finite life

that of the pure ML models. However, given the high cost of data collection in DED, PIML achieved comparable accuracy with only 20 % of the data required for training the deep neural networks.

The basis of the above-mentioned studies in using PDE-related terms in the loss function of ANN in PIML models is to use a set of collocation points. Hosseini et al. [141,142] proposed physics-inspired non-homogeneous methods for selecting collocation points to improve the efficiency and accuracy of the model. They developed an ANN-based PIML model for predicting the temperature and meltpool dimension in a single-track PBF process using space coordinates, time, laser power, laser scanning speed, thermal conductivity, and specific heat capacity as inputs. Unlike traditional grid-based approaches, their ANN-based PIML is grid-free and aims to minimize the residuals of the heat transfer PDE and its initial and boundary conditions for selected collocation points. Results showed that PINNs were 5 to 6 orders of magnitudes faster than the FEM method, with a storage size of just a few megabytes for the entire range of process-material parameters, while FEM simulations could require several gigabytes for each scenario.

Data generation can also be done by using voxels in the domain and calculating physical parameters for each of them. A CNN-based PIML that utilizes the transient 3D heat equation to simulate temperature changes in a solid object over time is reported in [143,144]. A voxel representation for PBF finite difference method is studied by considering the temperature and heat generation values at each voxel at a given time as inputs, and the estimated temperatures of the voxels at the next time step as outputs. The loss function integrated temperature values in the voxels, taking into account the corresponding conduction, convection, and heat generation effects. To maximize the efficiency of generating training data while minimizing the potential for researcher-selected bias, a stochastic method was used. The researchers used the Wilcoxon signed-rank test to determine that, in general, the PIML outperforms the label-trained ANN when trained on the same data and constraints. A CNN-based PINN for porosity prediction in LMD process has been developed in [147], by using various combination of physical variables such as maximum melt pool temperature, melt pool length and width in loss function. Furthermore, reality-augmented data can enhance the performance of PINNs, as proposed by Zhu et al. [153]. The augmented data was obtained from a limited number of experiments and an accurate 3D heat transfer model that includes turbulence. The results showed that this approach achieved higher efficiency compared to simulations.

In addition to the previously discussed hyperparameters and convergence methods, the variables within the physical models play a crucial role in achieving high accuracy. The accuracy of PINNs depends on the parameters in the governing physical equations, such as temperature-dependent thermal properties and specific heat, which are often difficult to measure experimentally. However, PINNs can identify these thermophysical properties using an inverse approach. Sharma et al. [149] introduced a forward-inverse PINN for the LPBF process. In the forward problem, a neural network uses temperature data from collocation points to predict velocity and pressure at those points. For the inverse problem, the neural network estimates the Peclet and Reynolds numbers using temperature and velocity data. It was found that the PINN model can infer unknown parameters like the Reynolds and Peclet numbers when provided with sufficient velocity and temperature

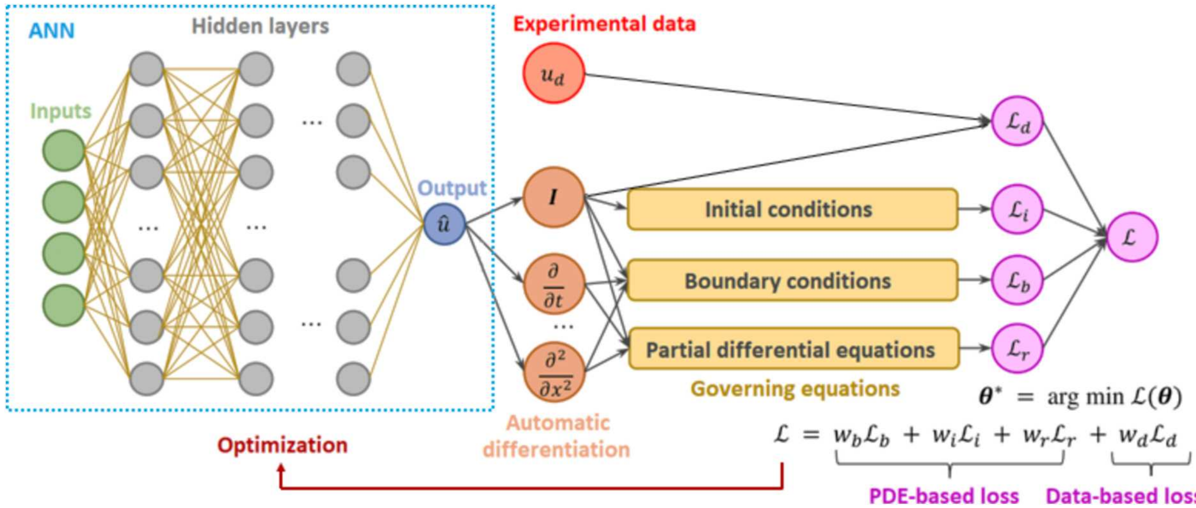

Fig. 18. PIML framework based on ANN with PDE-related and data-based loss function [132].

training data.

Eventually, most of the discussed studies are focused on developing PINN for single-track prints. In practice, it is fundamental to extend the solutions from single-track scenarios to various manufacturing conditions, multi-track prints, and part-level results. Li et al. [136] developed a transfer learning part that allowed for faster predictions without sacrificing accuracy when dealing with different manufacturing scenarios. The computational time required for this approach was approximately one-third that of FEM. An extension of PINN for multi-track PBF prints indicated temperature discrepancies of less than 7 % and meltpool size differences of under 1 % when compared to FEM simulations [137]. By using the transfer learning of a pre-trained PINN for a PBF print layer, Uhrich et al. [138] tuned the weights for the next layers with a considerably lower time. It was shown that the PINN model can be used to study thermal stresses by evaluating the temperature gradients predicted by the PINN model.

3.3.2. Using physics-based parameters in the loss function

Another way of fusion of data in loss function is by incorporating domain knowledge and physics-based parameters rather than using PDE residuals. This helps to constrain the loss function or penalize the network while training and eventually guarantees the physical soundness of the PIML model. To do so, an ANN-based PIML framework is employed by Salvati et al. [151] to predict finite fatigue life in materials containing defects. They developed a linear elastic fracture mechanics semi-empirical model to represent the physics of the problem and fused it within the loss function of the PIML model. From the semi-empirical model, the two-sided confidence intervals are fused as constraints with the regular neural network's loss function. They employed limited experimental data from the literature to create and validate the model's accuracy for the AlSi10Mg alloy produced by the PBF method. Incorporating a physical model as an additional constraint in the loss function represents a significant step towards developing more interpretable models, as opposed to traditional models that are based solely on available data. As shown in Fig. 19, a combination of physical loss and data loss is utilized in the proposed PIML model. The PIML model demonstrated an 83 % improvement in R^2 compared to the traditional ML model that relied solely on data loss without any physical constraints.

Kapusuzoglu and Mahadevan [145] developed an ANN-based PIML model that can predict the overall dimensionless neck diameter and porosity of MEX parts. Three techniques were presented for merging physical knowledge into a PIML. The first method involves integrating physical constraints into the loss function of the PIML. The second approach uses physics model outputs as supplementary inputs to the PIML model. The third technique involves pretraining a PIML model with physics model input-output data and then fine-tuning it with experimental data. The loss function includes physical violations related to the overall dimensionless neck diameter and porosity, as well as the physical relationship between mechanical properties and neck diameter. Eight different combinations of the above-mentioned three techniques were explored using printer extrusion temperature, speed, layer height, filament width, length, number of layers, and number of filaments per layer as model inputs. It was demonstrated that incorporating physics knowledge not only enhances prediction accuracy and produces physically meaningful results but also enables accurate model predictions with smaller amounts of experimental data. However, if the physical model is computationally expensive, the advantage of the pre-training technique in using a larger input dataset gets restricted.

3.4. PIML models with more than one fusion mechanism

Integrating thermal simulations, sensor data fusion, and data-driven approaches has been one of the promising research directions in recent years [154,155]. While not frequently explored, it may be possible to form PIML models where multiple fusion mechanisms discussed above are integrated together. For example, Ciampaglia et al. [150] created a PIML model based on both loss function modification and architecture shaping approaches that predict how process parameters impact the fatigue response of AlSi10Mg specimens made through AM. Two neural networks were first used in parallel to predict the defect and to estimate the microstructure. In the defect estimation neural network, the effect of build orientation, hatch, speed, energy, power, layer thickness, beam diameter, and plate temperature on the predicted defect size was studied. In Microstructure estimation, duration and temperature of the thermal treatment were used to predict the microstructural strength parameter. Next, the ratio of the defect and microstructure results were combined in a loss function of the ANN-based PIML model to predict fatigue strength. The models were trained using experimental data from the literature. PIML performance was compared with a common feed-forward neural network, and it was shown that the PIML model is in agreement with the experimental data, with mean and maximum errors of 4 % and 17 %, respectively. It was concluded that the proposed model allows designers to directly assess fatigue strength from process parameters and heat treatment properties without the need for time-consuming and expensive experimental fatigue tests. The proposed approach also proved promising in optimizing part design for the best fatigue performance.

To provide a real-time PIML model, Sajadi et al. [156] developed a PIML model for temperature prediction in metal additive manufacturing by implementing physics-informed online learning. This model utilizes physics-informed inputs and loss functions to dynamically update its weights as new, unseen data becomes available. This continuous adaptation enables the model to refine its predictions in real-time, showcasing significant potential for enhancing the online control and optimization of metal AM processes. Physical knowledge can also be fused to the model inputs, architecture, and loss function, simultaneously. Wang et al. [146] developed a probabilistic PINN model for uncertainty-aware fatigue-life prediction of PBF-fabricated parts. The neurons and loss functions were constrained by physical laws and physical models, respectively. Consequently, the reliability interval for predicting fatigue life using a parameterized approach in probability and statistics was assessed by generating the average prediction curve and confidence limits for fatigue life.

4. Summary and scope for future work

In this section, first, the reviewed studies on PIML for PSP modeling in AM are visually categorized and explored based on various factors, including the considered AM technology, adopted ML model, integration methodology of physics into different stages of ML models, source of the physical knowledge, and targeted parameter/output in either of the process, structure, property categories. The aim of these visual summaries and discussions is to provide an overview of the focus of the current literature, while simultaneously revealing potential discernible gaps, e.g., scarcity of PIML studies targeting a particular AM process. Next, additional discussions on the consideration of developing PIML models, technical research gaps, and potential future research directions and challenges are presented.

4.1. Summary of the reviewed PIML studies

This section highlights the summary of reviewed PIML models from different perspectives based on AM technologies, ML models, sources of physical knowledge, and PSP relationships.

4.1.1. Summary of PIML studies based on AM technologies

According to Fig. 20, the majority of the reviewed PIML studies focus on metal-based AM technologies, including powder-bed fusion and directed energy deposition processes. PIML modeling for polymer-based AM techniques, which generally rely on different physical principles as metal-based processes, such as material extrusion and vat photopolymerization processes, are also explored, but they are not studied as much as metal-based AM methods. The emphasis on metal-based AM processes finds its rationale in the strategic significance that metal components hold across industries, most prominently in sectors like aerospace and automotive. Consequently, accurate prediction and control of the product quality using powerful and emerging techniques such as PIML is crucial. On the other hand, this highlights a potential gap in exploring PIML models and applications in other AM technologies, such as binder jetting, material jetting, and sheet lamination, as well as expanding studies on the less explored AM categories, including vat photopolymerization.

Another observation from Fig. 20 is that while all three categories of physics fusion techniques, namely feature engineering, architecture shaping, and loss function modifications, have been utilized to implement PIML models for different AM technologies, physics-based feature engineering has been the most common approach among researchers. This preference can likely be attributed to its inherent implementation simplicity compared to other approaches. The architecture shaping method is, however, the least explored approach as it generally requires a deeper understanding of both the underlying physics, the intricacies of the model architecture itself, and clear methodologies for integration.

4.1.2. Summary of PIML studies based on ML models

Fig. 21 illustrates the distribution of different ML models that have been explored by researchers in the field of PIML for PSP modeling in AM. As expected, ANNs are the most commonly used method and have been examined in all three categories of feature engineering, architecture shaping, and loss function modifications. The analysis indicates that physics-based feature engineering techniques are applied with a broad range of ML models, including neural networks, tree-based models, GPR, KNN, SVM, and different linear ML models. However, the categories of architecture shaping, and loss function modifications were solely studied on neural networks and deep learning models. This points to a research gap in incorporating physical knowledge into the architecture and training processes of a broader range of ML models, rather than limiting the focus exclusively to neural networks.

A heat map of the reviewed PIML studies based on the focused ML models for different AM technologies is shown in Fig. 22. It can be seen that ANN models are the most widely studied models in all AM processes. While a variety of classical ML models were reported for the PBF process, the other AM technologies, such as DED, MEX, and VPP mostly considered deep learning as the ML component of their PIML models. Although, the latest advanced ML models such as neural operators have been implemented in AM field [157], there is a research gap in exploring physics-informed versions of neural operators [158] and transformer-based PINNs [159] within the scope of AM.

It is worth mentioning that irrespective of the chosen ML model, to get the best accuracy, the hyperparameters of the model should be tuned appropriately [160]. According to the reviewed articles, trial and error method is widely used for tuning the hyperparameters. By trying different combinations of hyperparameters [106], using cross-validation [98], grid search method [140], and implementing sequential Bayesian optimization [94], the best combination of the hyperparameters can be chosen to get the desired accuracy.

4.1.3. Summary of PIML studies based on the target output in the PSP chain

Given the scope of the current study, i.e., PIML for process-structure-property modeling in AM, the target of interest for all studies has been to provide predictions on components related to either of the process (e.g., meltpool dynamic, thermal profile), structure (e.g., microstructure and pores), or property (e.g., tensile strength, dimensional accuracy) of additively manufactured components. A summary of the studies based

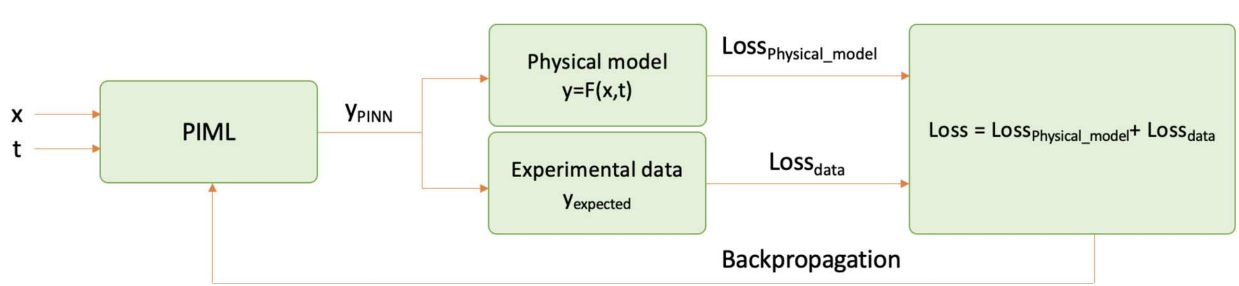

Fig. 19. Using physical model in the loss function (Reproduced with modifications from [151]).

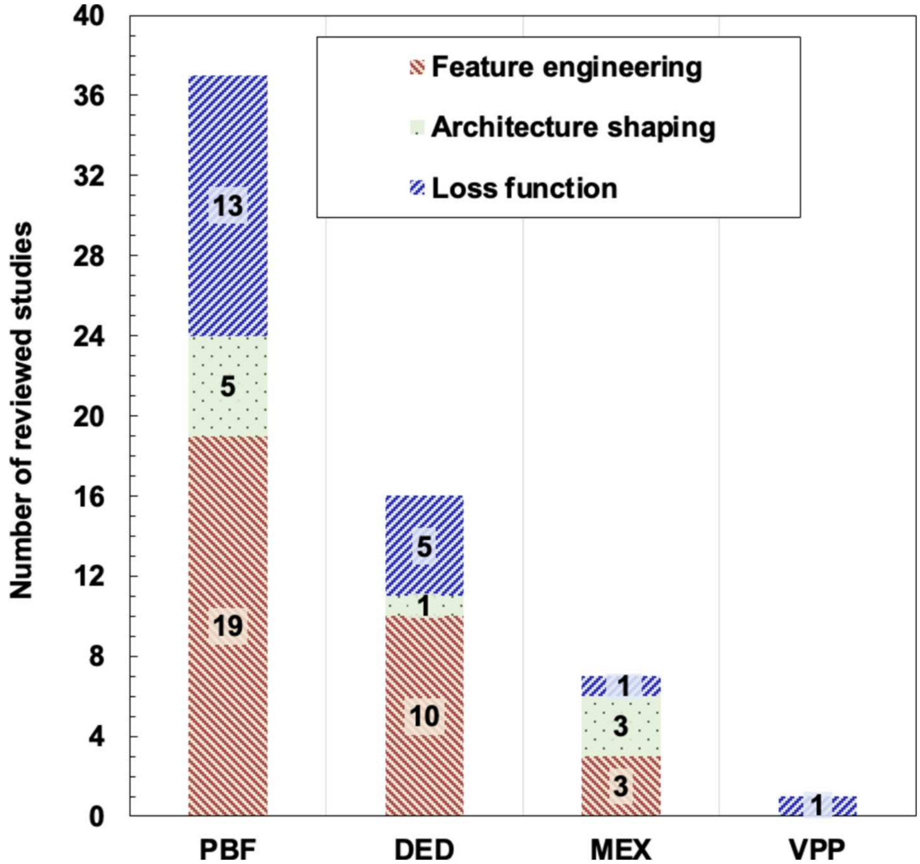

Fig. 20. The number of reviewed studies on developing PIML models for different AM technologies.

on the category of the targeted output is provided in Fig. 23. It can be seen that while all three physics-fusion mechanisms have been considered in these studies, the prevalent fusion method utilized for all three PSP categories is feature engineering, followed by modifications to loss functions and architecture shaping.

According to Fig. 23, the process class is the most extensively studied category, accounting for over 50 % of the total studies. This prominence can be attributed to the availability of numerous process-related variables, such as input process parameters [91,111] or process signatures like thermal behavior [120,134,135,161], meltpool size [98,141], meltpool dynamics [139], thickness [121]. These variables can be measured/estimated experimentally or obtained by solving governing equations. Feature engineering approaches primarily target process-related parameters, while modifications to architecture and loss functions are typically employed when governing equations are accessible. For structure predictions, researchers aimed at using PIML models to get the porosity [94,110,145], pore size [88,109], grain structure [87,123], balling defects [85], crack formation [86] in different AM processes. Eventually, the property-related parameters like tensile strength [96,106,124], yield stress [106], fatigue life [150,151] were obtained using PIML models. Since the current modifications to architecture shaping and loss functions mainly rely on established governing

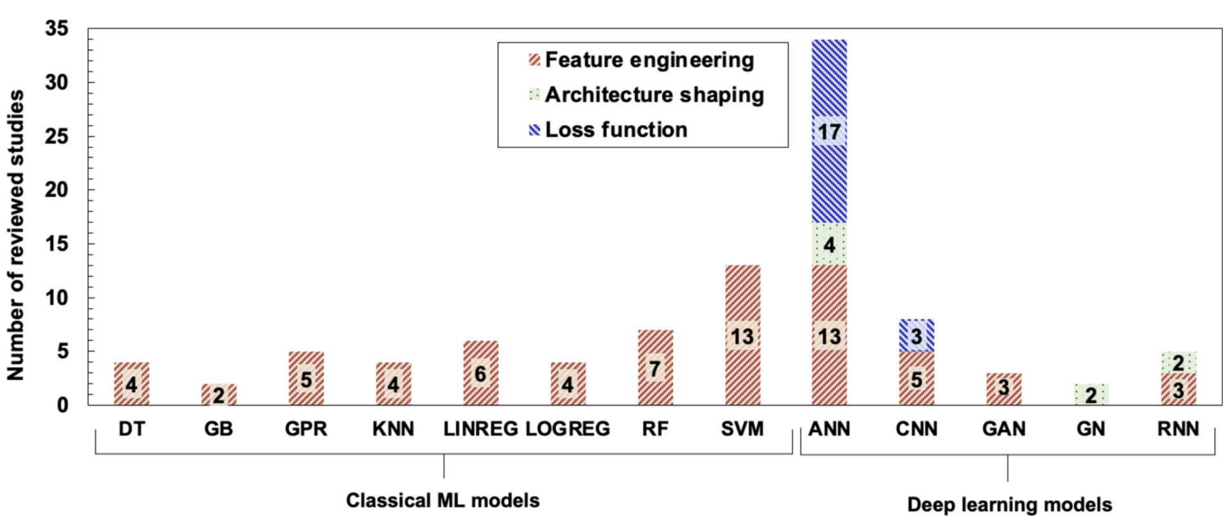

Fig. 21. Number of reviewed studies versus different ML methods used in PIML modeling of AM technologies.

equations, most studies predicting structure-related and property-related factors predominantly use physics-informed feature engineering.

In addition to PSP discovery, PIML frameworks can be utilized for process optimization, design, and control in AM. For example, PINN can predict thermal fields in metal AM across different process parameters, helping to determine optimal processing conditions. On the design side, methods such as physics-informed geometric operators [162] can be applied to enhance the efficiency and accuracy of the AM design process. Moreover, PIML methods offer the capability to integrate real-time sensor data and dynamically update models for more accurate control and adjustments [50,163].

4.1.4. Summary of PIML studies based on the source of physical knowledge

As previously discussed, sources of physical knowledge used to fuse into PIML models can stem from different origins, including (i) governing physical equations, (ii) data-centric approaches without using any physical equations, or (iii) both through a hybrid mechanism. As depicted in Fig. 24, studies based on data-centric approaches to derive physical knowledge mainly adopt a feature engineering mechanism to fuse that physical knowledge with the ML model. On the other hand, the majority of loss function-based fusion mechanisms rely on governing physical equations as the source of physical knowledge. This highlights that mechanistic and physical models play a bigger role in how ML models learn, while physical knowledge derived through data-centric approaches may be more valuable for identifying features that may contribute to the output.

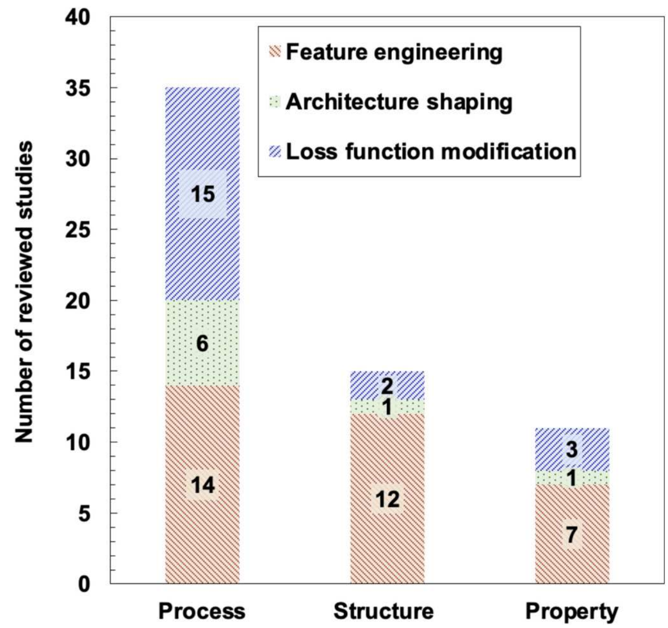

Fig. 23. The number of reviewed studies versus PIML predictions related to PSP parameters.

4.2. Challenges, research gaps, and directions for future research

This section highlights the current challenges, research gaps, and potential future directions with respect to PIML for PSP modeling in AM.

4.2.1. Computational time for PIML models

In addition to the accuracy of PIML models, the computational needs and time of PIML models should also be considered. In general, the required time of a model depends on the adjustment of different parameters and should be considered along with the model accuracy in cases where a trade-off exists between them. For example, in the case of loss function modification, the PIML model was 5 to 6 orders of magnitude faster than FEM simulations in [141], while it was two times slower than FEM models in [139]. Therefore, it is beneficial to consider different factors that might impact the computational times.

One factor that affects the computational time is the number of input features. As seen in feature engineering approaches, an increment in the number of features might increase the complexity of models and so correspondingly increase the running time [100]. For example, compared to CNN, using the SHAP-based PIML model reduces the computational time from 5.8 s to only 1.2 μs [106]. On the other hand,

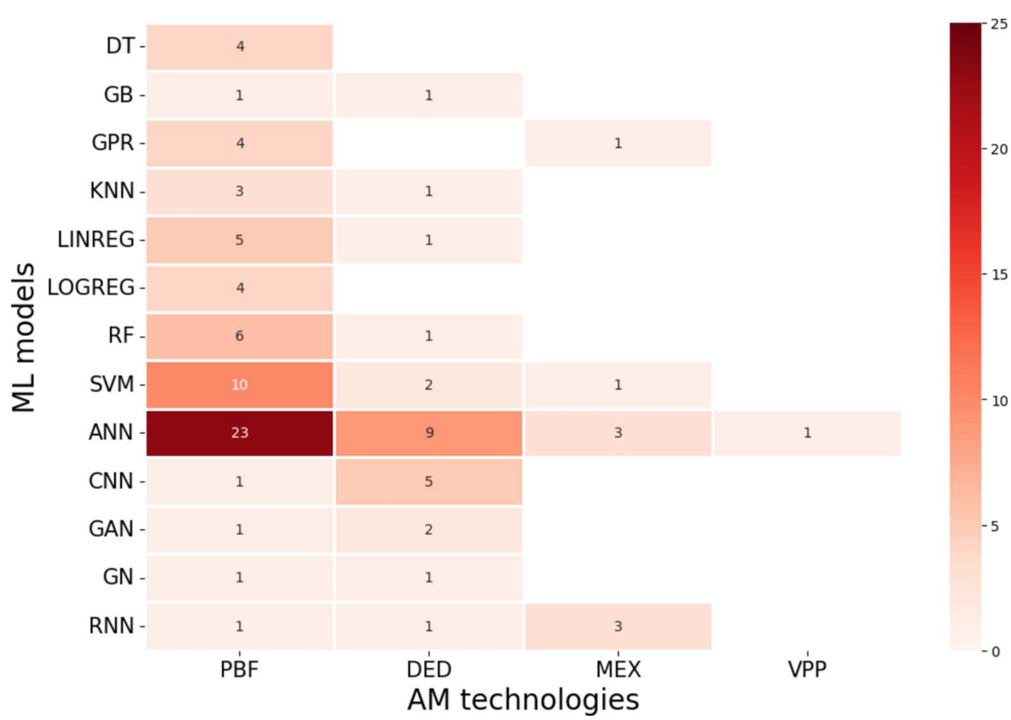

Fig. 22. Heat map representation of ML algorithms used in PIML modeling of different AM technologies.

augmented features can be used to build up more causal PSP relationships. Therefore, it is necessary to use appropriate feature engineering techniques to attain higher accuracies as well as lower computational needs.

Another factor that affects the computational time is the chosen machine learning model. It was reported that by using deep unfolding technique in the architecture of a PIML model, higher accuracy can be obtained compared to ANN, ETR, LSTM, and SVR models [120]. While its training time is lower than that of ANN and LSTM, it takes more time than ETR and SVR to train. This difference might be attributed to the fact that unfolding the physics-based equation in the model architecture helps to have a sparse network and faster training compared to the fully connected ANN and LSTM [120].

Another factor affecting computational time is the programming tool used to build the machine learning part of PIML models. In the reviewed papers, machine learning models are mainly implemented in Tensorflow [91,118–120,135,136,139,140,143] and Pytorch [125,132,141,145,151]. Due to the large and complex matrix calculations, the selection of appropriate coding libraries can significantly impact the training time of the model as well as simplify the implementation. For instance, in cases that deal with PDEs, utilizing the automatic differentiation capabilities of specific libraries in Python can facilitate the performance.

Finally, it is important to mention that computational time is also dependent on the computational power, i.e., central processing unit (CPU) and graphics processing unit (GPU). As most of the reviewed papers didn't report the computational time and power, it is recommended that details in terms of computational needs and time be provided in future studies to better evaluate the PIML models and their applicability in various scenarios, such as real-time AM control. As conventional physics-based models are usually time-consuming, PIML models can be a leading approach in the real-time investigation of AM processes. Inspiring from the research on in-situ monitoring of AM processes using ML [43,45,164], further integration of real-time process monitoring and defect detection with PIML models appears to be beneficial.

4.2.2. Dataset size and data availability concerns in PIML models

Data availability is one of the main issues of machine learning models, especially in the field of AM. Thanks to the knowledge coming from physics, PIML models are reported to be less data-hungry compared to pure machine learning models [99,118–120,133,151]. Table 3, Table 4 and Table 5 provide a summary of the type of input data and different dataset sizes for different PIML models based on various fusion mechanisms and sources of physical knowledge. For example, the studies using images reported dataset sizes of 1500-118 k, and the collocation points generated for loss function modifications were in the order of 100 k-10 M. In most of the reviewed papers, the sample sizes (data points) typically ranged from around 26 to 3318, while the number of experiments (from which data points were extracted) varied between approximately 5 and 144. This highlights the importance of developing a standardized outline for reporting the dataset size and its details in future PIML studies in the field of AM. Moreover, as the AM field is getting mature, providing guidelines for building on open-access database brings significant advantages to establish future PSP-related frameworks [53].

The datasets in PIML studies were provided using various experimental approaches and numerical simulation tools such as Abaqus [136], Autodesk Netfabb [98], FEniCS [132], Matlab [100,135], OpenFOAM [91], etc. As using simulation software and in-situ data collections are complex, cost-prohibitive, and time-consuming,

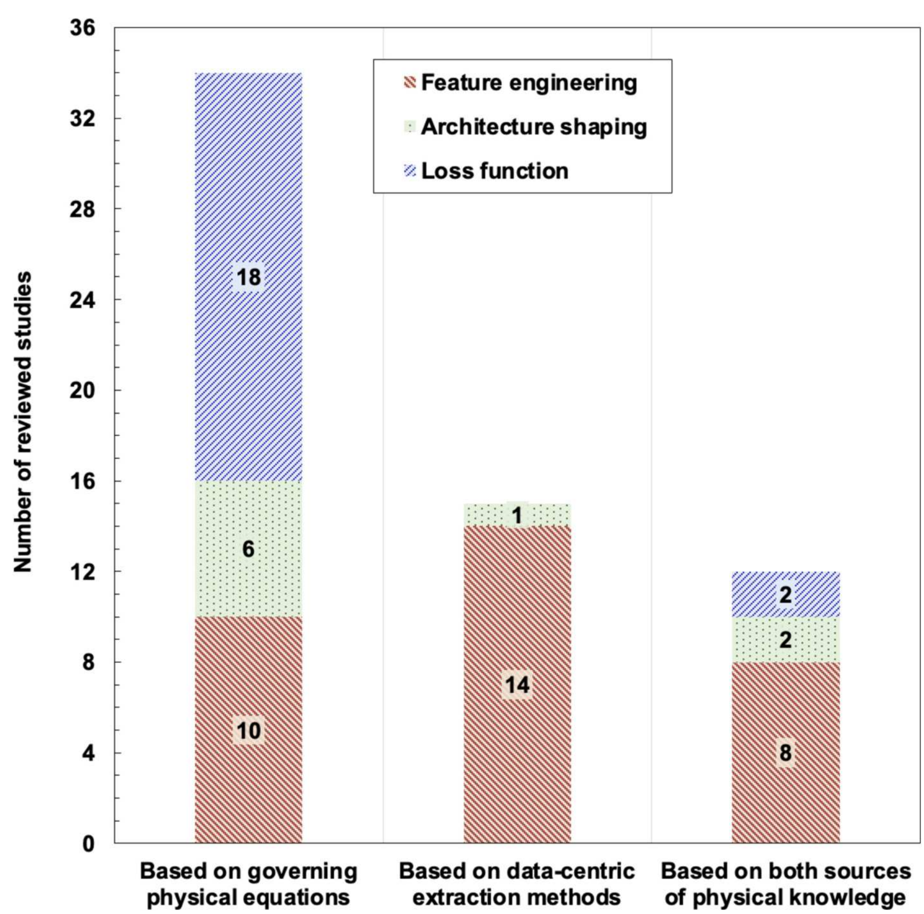

Fig. 24. The number of reviewed studies versus the sources of physical knowledge fused into PIML models.

generative AI techniques are becoming a promising solution to provide the data for ML models. Generative adversarial networks [165], diffusion models, and VAE [166] are among the most popular generative AI models in various domains. These models can be further fused with physical knowledge, e.g., physics-informed conditional GANs, to generate additional data required for training PIML models [167]. Future studies on developing physics-informed generative models in AM can pave the way for further development of PIML models.

4.2.3. Generalizability and transferability of PIML models

It is important to consider the potential generalizability of established PIML models to various AM machines, different materials, and complex print geometries. Transfer learning can be considered as a suitable method to perform this generalization. For instance, by using transfer learning to extend the modified loss PIML framework to various manufacturing parameters, simulation time was reduced to only 1/3 of the FEM simulation time [136]. In another study, knowledge transfer was used on a PIML model to predict the performance for various conditions and 3D printers [99]. More details on the implementation of transfer learning in modeling AM processes can be found in a review done by Tang et al. [168]. The transfer learning concept can be further integrated into PIML models in future studies.

To formulate generalizable PIML models, researchers have been working on extended physics-informed neural networks through physics-based loss function modification [169]. The extended physics-informed neural networks can solve forward as well as inverse PDE problems, which will improve understanding of PSP relationships and generalize ML models for more applications. The AM community can thus leverage such advancements and explore these novel approaches to establish generalizable PSP models as a future direction.

Moreover, reinforcement learning has emerged as a promising approach to enhancing the generalizability of machine learning models. By learning from interactions with environments and optimizing actions based on reward signals, reinforcement learning models can develop more robust representations that capture underlying patterns in the data. Although reinforcement learning has been used to optimize printing path control function [170] and minimize the defects [171] in the field of AM, there is a research gap in PIML modeling of AM processes using reinforcement learning. Therefore, physics-informed reinforcement learning can be brought into the field of AM in future studies, as similar efforts are made in other domains, such as wireless navigation [172] and connected automated vehicles [173].

Exploring the integration of federated learning, a machine learning approach that enables multiple entities to collaboratively train a shared model without having to share their raw data with each other, and physics-informed learning can be an interesting topic of future research and may hold several potentials for increasing the generalizability of PIML models. [174]. For example, additive manufacturing processes may be executed by different manufacturers or distributed across various geographical locations. Each entity might have data specific to its environment and conditions. Federated learning could facilitate the collaboration of these entities to jointly train a physics-informed model that captures and updates the models based on physics. Additionally, different computing models, such as edge computing [175], can also be fused with PIML methods to increase the generalizability of models [176].

4.2.4. Interpretability, explainability, and trustworthiness of PIML models

The interpretability, explainability, and trustworthiness of PIML models represent critical considerations in ensuring the effectiveness and reliability of their application for the AM community. The interpretability and explainability factors refer to the model's capacity to provide transparent and interpretable insights and rationale into its decision-making processes. This transparency is extremely important for the AM community because it helps human users trust and believe in the model's results, specifically given their critical application domains. While these topics have been long an important area of research among artificial intelligence researchers, the emergence of PIML models has opened up new directions of research for the community [177].

Although it may seem logical that adding physical knowledge to machine learning models would automatically enhance their interpretability and explainability, the situation is often more complex and requires deeper analysis. In reality, the interpretability and explainability of physics-informed machine learning (PIML) models depend on factors such as the model architecture, how data is represented, and the methods used to integrate physical knowledge. Therefore, not all PIML models offer a similar level of explainability and interpretability [178]. For example, while leveraging physics during the ML model training through loss function modification (e.g., in PINNs), can help capture underlying physical behaviors, it still suffers from lack of interpretability at the model architecture level. There has been some ongoing research on enhancing the explainability of physics-informed models through, e.g., using PCA to explain distributed representations [179] and performing sensitivity analysis [180]. Enhancing the interpretability of PIML models by methods such as Kolmogorov Arnold Networks [56], and Sparse PINNs [55], etc. remains a highly active and prominent area of ongoing research [54].

On the other hand, fusing the physical knowledge into the architecture of ML models may hold a higher promise in formulating more explainable models. For instance, in a recent study that employed architecture shaping through the deep unfolding approach to predict thermal history in the PBF AM process [120], the neural network's weights and biases were intricately linked with physical model parameters and coefficients. Consequently, after the model has been trained, it becomes feasible to precisely extract these physical model coefficients, often linked to material properties. This approach carries substantial importance, as it allows for a more profound understanding of the model's behavior and provides a clearer pathway for relating predictions to the real-world factors they represent, thus enhancing model interpretability and explainability.

There is a significant research gap when it comes to investigating and improving the explainability of PIML models within the AM community. As interpretability and explainability are subjective in nature, the gap becomes even more pronounced, especially considering the critical role that process-structure-property modeling plays in AM. Striking a balance between PIML model complexity, predictive accuracy, and interpretability remains an ongoing challenge that necessitates careful design and optimization. Within the context of PIML model trustworthiness, it is also important to establish new criteria, standards, or metrics based on process physics, available process data, and model characteristics that guide human users in placing confidence in the model's predictions.

4.2.5. Fusion of physical knowledge and its challenges in PIML models

Although there are several approaches to integrating physical knowledge with the ML models, each may offer several advantages while suffering from limitations. These capabilities and challenges have been summarized in Table 6 and may be used by researchers to identify the appropriate fusion mechanism. It can be seen that in general, based on the available data and source of physical knowledge, appropriate physics fusion methodology can be selected. However, selecting the fusion approach might require some considerations, such as access to appropriate software, coding skills, and computational power, for example.

4.2.6. Multi-modal PIML: integrating various fusion mechanisms

Multi-modal PIML models can be considered as PIML models in which various sources of physical knowledge are fused into different stages of the machine learning model. As different physical sources and fusion mechanisms offer various capabilities in PIML models, multi-modal PIML models are expected to perform better than existing PIML models. For instance, architecture shaping fusion approaches can be mixed with loss function fusion approaches, or feature engineering

Table 6
Challenges and capabilities of various physics fusion methodologies for PIML modeling in AM.

Fusion approach	Capabilities (Implementation and performance)	Challenges/Limitations (Implementation and performance)
Physics-based feature engineering	• Can be employed even when specific physical models or equations are not readily available, by efficiently obtaining underlying physical insights through data-centric feature engineering. • Are generally more straightforward in implementation. • Most insightful physical features can be identified and incorporated into the model using various feature engineering methods.	• Pre-processing (e.g., through image analysis, machine learning, and statistical analysis) might be required to obtain the desired physical knowledge. • As physical fusion is done only for the model inputs, the black box nature of the ML part still exists, limiting the interpretability of this technique.
Physics-based architecture shaping	• Parameters in the model architecture (e.g., weights) can be guided directly by physical knowledge, resulting in time-efficient and data-efficient training. Thus, they may be beneficial for data-scarce scenarios. • Can generally create more explainable models. For example, the weights attached to physical parameters in the deep unfolding architecture shaping methods can give more accurate information about changes in the physical parameters. Besides, physical equations can be considered as weights of the causal graph network, leading to a faster training process. • As the model architecture consists of physical equations, these models may easily be transferred and generalized for certain problems but with different processing parameters and materials. • Certain models, such as knowledge graph have the capability to link the entire PSP chain.	• The coding part of fusing the physical equations into the architecture of machine learning models might not be straightforward. Therefore, more advanced knowledge of using appropriate software/coding libraries for integrating physics into ML architecture is necessary. • The form of required physical equations to be compatible with a certain architecture shaping approach may be subject to constraints [120].
Physics-based loss function modification	• Governing differential equations can be fused to the loss functions and solved using the automatic differentiation capabilities of ML libraries. • Semi-empirical and physical parameters can be integrated into the loss function to constrain the solution domain based on physical knowledge. • As they can be trained with no/limited data, they can be considered as data-efficient approaches compared to pure ML models. • The solutions for a specific case can be transferred and generalized for different processing parameters and materials.	• The development of PIML models with modified loss functions may face challenges in terms of computation time and required resources. • In addition to collocation points generated for solving PDEs, additional data terms are usually required for increasing the model accuracy and reducing the training time.

methods can be combined with modified loss functions to form more interpretable models with higher prediction accuracies. For example, Kapusuzoglu and Mahadevan [145] developed a PIML model that incorporates physical knowledge into the loss function to predict bond quality and porosity in fused filament fabrication parts. Additionally, the outputs from the physical model are used as extra inputs to the network, creating a hybrid PIML model that leverages physics both as input features and within the loss function. Their findings indicated that this hybrid approach outperforms the strategy of solely embedding physical knowledge in the loss function. Surprisingly, not many researchers have looked into this idea of blending different fusion methods together, especially in the field of AM and PSP modeling. Identifying when and how to mix different fusion approaches to maximize their synergies is an important and exciting direction of research, yet to be explored.

4.2.7. Usefulness and suitability of PIML models

In general, it is without doubt that PIML models and the ongoing research by the research community hold significant promise in enhancing ML model predictions and accuracy by connecting them to the physical laws. However, the decision on whether to use PIML models or not could be subject to discussion in a case-by-case scenario and would be of significance to AM practitioners.

There are several circumstances that using a pure ML model may suffice for a given application. For example, if there is an ample amount of high-quality data available, exploring PIML models may not be justified. Nonetheless, in the context of AM, this may pose significant experimental cost and burdens. Additionally, even if the dataset is sufficiently large but does not adequately represent the entire domain, PIML models may be more suitable as they are constrained with physical knowledge compared to the pure ML models that only rely on training data. Unlike pure ML models that rely solely on training data, PIML models incorporate physical knowledge, making them better equipped to handle diverse conditions and provide more reliable insights. On another note, if the underlying physical model used to inform the PIML framework is inherently flawed, the performance of the PIML model may suffer compared to pure ML models. This is because the PIML model relies on embedding physical laws as prior knowledge, and when those laws are inaccurate or incomplete, the PIML model may be constrained by inaccurate assumptions. In such cases, leveraging inaccurate physics can hinder the model's predictive capabilities, while purely data-driven ML models could perform better by relying solely on patterns learned directly from a large set of data.

Furthermore, the risk and quality acceptance threshold for various AM applications and products may be different and needs to be carefully considered when evaluating the suitability of pure ML models versus PIML models. Developing standardized benchmarks and metrics tailored to PIML approaches would be highly beneficial, taking into account the varying contributions of experimental methods, numerical simulations, and machine learning models. This should include evaluating factors such as data collection costs, computational requirements, and overall process effectiveness from data acquisition to target prediction and, perhaps real-time applications. Moreover, recently, there have been some emerging efforts in the certification of deep learning models (which perhaps can be extended to PIML approaches in the future), particularly focusing on the training process to evaluate whether a model has been properly trained using the available data. These efforts aim to provide systematic, data-aware methods for assessing training quality and ensuring the reliability of neural networks [181]. Therefore, a comprehensive comparison framework would allow for a fair assessment of different PIML methods and empower researchers to utilize these approaches more effectively.

5. Conclusions

Physics-informed machine learning methods have distinct potential to enhance interpretability, robustness, and computational tractability towards the prediction of critical process-structure-property relationships in AM. Incorporating the fundamental physics of AM processes into ML models overcomes the drawbacks regarding the high computational cost of physics-based simulations, as well as high data requirements and lack of interpretability pitfalls of black-box ML models.

In this review, different physics-informed approaches towards PSP modeling in AM using a wide variety of machine learning models and physical knowledge sources are summarized. The reviewed PIML studies are grouped into three main categories including feature engineering, architecture shaping, and loss function modifications. The following highlights can be drawn from different viewpoints of the reviewed studies:

- Physics-based feature engineering for PIML models: The feature engineering category includes the generation of physics-informed variables based on analytical models and numerical simulations, the extraction of physical knowledge by various data-centric methods such as statistical approaches, image analysis techniques, and multi-stage ML models, as well as the combination of different data sources, feature mapping, and feature selection techniques.
- Physics-based architecture shaping for PIML models: The architecture shaping category includes innovative approaches to fuse physical knowledge into the architecture of ML models rather than using pre-defined off-the-shelf ML models. The development of physics-informed causal graphs, graph networks, LSTM networks, and deep unfolding methodology is among the latest PIML architecture shaping research studies.
- Physics-based loss function modification for PIML models: Loss function modification using physics knowledge is done by incorporating residuals of governing differential equations or by using physics-based parameters in the loss function.
- Sources of physical knowledge in PIML models: The sources of physical knowledge fused in different stages of PIML models can be based on either governing physical equations such as analytical models, governing PDEs and numerical simulations, or various data-centric techniques including statistical methods, data augmentation techniques, image analysis tools, and multi-stage ML models. Moreover, a combination of both sources of physical knowledge integrated into various stages of PIML models, i.e., feature engineering, architecture shaping, and loss function modification, are pursued in the literature.
- Multi-modal PIML models: In general, based on the type of available data and physical knowledge, appropriate fusion methodology can be chosen for PIML models. As a future research direction, various sources of physical knowledge can be fused in different stages of the PIML models to create multi-modal PIML models.
- Additive manufacturing technologies examined by PIML models: Regarding the AM methods, various PIML models were developed for PBF, DED, MEX, and VPP processes. Based on the existing body of knowledge, PBF has gained significant attention in the AM community, followed by DED and MEX processes. However, there is a research gap in the development of PIML models for binder jetting, material jetting, sheet lamination, and vat photopolymerization AM methods.
- Machine learning models used in PIML modeling of AM technologies: In terms of machine learning models, ANNs are the most used method and were examined in all three categories of feature engineering, architecture shaping, and loss function modifications, as well as in all AM processes. The review showed that physics-based feature engineering techniques are developed based on various ML models, including neural networks, tree-based models, GPR, KNN, SVM, and different regression-based parametric models. However, neural networks are the only approach used in reviewed architecture shaping and loss function modification studies. While a variety of classical ML models were reported for the PBF process, DED, MEX and VPP methods were mostly studied with deep learning PIML methods.
- Interpretability, explainability and generalizability in PIML models: The level of interpretability and explainability in PIML models can be impacted by factors such as the type of data, source of physics, ML model architecture, and the particular techniques used to integrate physical insights. Consequently, there is variability in the extent of explainability and interpretability among different PIML models and further research is beneficial in obtaining more interpretable and explainable PIML models. To further extend the PIML models, more future research directions could be followed to generalize PIML models into various AM machines, different materials, and complex print geometries using different physics-based and machine learning models. Generalizability of PIML models can be done through different learning approaches such as transfer learning, reinforcement learning, and federated learning.

CRediT authorship contribution statement

Meysam Faegh: Writing – original draft, Visualization, Formal analysis, Conceptualization. **Suyog Ghungrad:** Writing – original draft, Formal analysis, Conceptualization. **João Pedro Oliveira:** Writing – review & editing, Methodology, Conceptualization. **Prahalada Rao:** Writing – review & editing, Methodology, Conceptualization. **Azadeh Haghighi:** Writing – review & editing, Supervision, Project administration, Methodology, Conceptualization.

Declaration of competing interest

The authors declare that they have no known competing financial interests or personal relationships that could have appeared to influence the work reported in this paper.

Acknowledgments

Prahalada Rao acknowledges funding from the National Science Foundation (NSF) via Grant numbers: CMMI-2309483/1752069, OIA-1929172, PFI-TT 2322322/2044710, CMMI-1920245, ECCS-2020246, CMMI-1739696, and CMMI-1719388 for funding his research program. Understanding the causal influence of process parameters on part quality and detection of defect formation using modeling, in-situ sensing and physics-based machine learning was the major aspect of CMMI-2309483/1752069 (Program Officer: Andrew Wells). JPO acknowledges funding by national funds from FCT - Fundação para a Ciência e a Tecnologia, I.P., in the scope of the projects Nos. LA/P/0037/2020, UIDP/50025/2020, and UIDB/50025/2020 of the Associate Laboratory Institute of Nanostructures, Nanomodelling and Nanofabrication – i3N.

References

[1] Gibson I, Rosen D, Stucker B, Khorasani M. Additive Manufacturing Technologies. n.d.
[2] Wang C, Tan XP, Tor SB, Lim CS. Machine learning in additive manufacturing: state-of-the-art and perspectives. Addit Manuf 2020:36. https://doi.org/10.1016/j.addma.2020.101538.
[3] Javaid M, Haleem A, Singh RP, Suman R, Rab S. Role of additive manufacturing applications towards environmental sustainability. Advanced Industrial and Engineering Polymer Research 2021;4:312–22. https://doi.org/10.1016/j.aiepr.2021.07.005.
[4] Sun C, Wang Y, McMurtrey MD, Jerred ND, Liou F, Li J. Additive manufacturing for energy: a review. Appl Energy 2021:282. https://doi.org/10.1016/j.apenergy.2020.116041.
[5] Lakshmanan R, Nyamekye P, Virolainen VM, Piili H. The convergence of lean management and additive manufacturing: case of manufacturing industries. Clean Eng Technol 2023:13. https://doi.org/10.1016/j.clet.2023.100620.
[6] Paek SW, Balasubramanian S, Stupples D. Composites additive manufacturing for space applications: a review. Materials 2022:15. https://doi.org/10.3390/ma15134709.
[7] Kaur I, Singh P. State-of-the-art in heat exchanger additive manufacturing. Int. J Heat Mass Transf 2021:178. https://doi.org/10.1016/j.ijheatmasstransfer.2021.121600.
[8] Mohd Javaid, Haleem A. Additive manufacturing applications in medical cases: a literature based review. Alexandria Journal of Medicine 2018;54:411–22. https://doi.org/10.1016/j.ajme.2017.09.003.
[9] Cheng H, Luo X, Wu X. Recent research progress on additive manufacturing of high-strength low-alloy steels: focusing on the processing parameters, microstructures and properties. Mater Today Commun 2023:106616. https://doi.org/10.1016/j.mtcomm.2023.106616.
[10] Kalia K, Ameli A. Understanding the process-microstructure-property relationships in material extrusion additive manufacturing of polylactic acid microcellular foams. Addit Manuf 2023:72. https://doi.org/10.1016/j.addma.2023.103636.
[11] Mostafaei A, Ghiaasiaan R, Ho IT, Strayer S, Chang KC, Shamsaei N, et al. Additive manufacturing of nickel-based superalloys: a state-of-the-art review on

process-structure-defect-property relationship. Prog Mater Sci 2023:136. https://doi.org/10.1016/j.pmatsci.2023.101108.
[12] Mostafaei A, Zhao C, He Y, Reza Ghiaasiaan S, Shi B, Shao S, et al. Defects and anomalies in powder bed fusion metal additive manufacturing. Curr Opin Solid State Mater Sci 2022:26. https://doi.org/10.1016/j.cossms.2021.100974.
[13] Buj-Corral I, Sivatte-Adroer M. An experimental investigation about the dimensional accuracy and the porosity of copper-filled PLA fused filament fabrication parts. Metals (Basel) 2023:13. https://doi.org/10.3390/met13091608.
[14] Pyeon J, Aroh Joseph, Jiang R, Verma AK, Gould B, Ramlatchan A, et al. Time-resolved geometric feature tracking elucidates laser-induced keyhole dynamics. n.d.
[15] Azarniya A, Colera XG, Mirzaali MJ, Sovizi S, Bartolomeu F, St Weglowski Mk, et al. Additive manufacturing of Ti–6Al–4V parts through laser metal deposition (LMD): process, microstructure, and mechanical properties. J Alloys Compd 2019;804:163–91. https://doi.org/10.1016/j.jallcom.2019.04.255.
[16] Nafar Dastgerdi J, Jaberi O, Remes H, Lehto P, Hosseini Toudeshky H, Kuva J. Fatigue damage process of additively manufactured 316 L steel using X-ray computed tomography imaging. Addit Manuf 2023:70. https://doi.org/10.1016/j.addma.2023.103559.
[17] AbouelNour Y, Gupta N. Assisted defect detection by in-process monitoring of additive manufacturing using optical imaging and infrared thermography. Addit Manuf 2023;67:103483. https://doi.org/10.1016/j.addma.2023.103483.
[18] Gillespie J, Yeoh WY, Zhao C, Parab ND, Sun T, Rollett AD, et al. In situ characterization of laser-generated melt pools using synchronized ultrasound and high-speed X-ray imaging. J Acoust Soc Am 2021;150:2409–20. https://doi.org/10.1121/10.0006386.
[19] Zagade P, Gautham BP, De A, DebRoy T. Analytical estimation of fusion zone dimensions and cooling rates in part scale laser powder bed fusion. Addit Manuf 2021:46. https://doi.org/10.1016/j.addma.2021.102222.
[20] Zagade PR, Gautham BP, De A, DebRoy T. Analytical modelling of scanning strategy effect on temperature field and melt track dimensions in laser powder bed fusion. Addit Manuf 2024:82. https://doi.org/10.1016/j.addma.2024.104046.
[21] Tan W, Spear A. Multiphysics modeling framework to predict process-microstructure-property relationship in fusion-based metal additive manufacturing. Acc Mater Res 2024;5:10–21. https://doi.org/10.1021/accountsmr.3c00108.
[22] Kamat S, Li X, Stump B, Plotkowski A, Tan W. Multi-physics modeling of grain growth during solidification in electron beam additive manufacturing of Inconel 718. n.d.
[23] Li X, Tan W. Numerical modeling of powder gas interaction relative to laser powder bed fusion process. J Manuf Sci E T ASME 2021:143. https://doi.org/10.1115/1.4048443.
[24] Li EL, Wang L, Yu AB, Zhou ZY. A three-phase model for simulation of heat transfer and melt pool behaviour in laser powder bed fusion process. Powder Technol 2021;381:298–312. https://doi.org/10.1016/j.powtec.2020.11.061.
[25] Yang Y, Li L, Zhao J. Mechanical property modeling of photosensitive liquid resin in stereolithography additive manufacturing: bridging degree of cure with tensile strength and hardness. Mater Des 2019;162:418–28. https://doi.org/10.1016/j.matdes.2018.12.009.
[26] Tayebati S, Cho KT. A hybrid machine learning framework for clad characteristics prediction in metal additive manufacturing. 2023. https://doi.org/10.48550/arXiv.2307.01872.
[27] Fang H, Ge H, Zhang Q, Liu Y, Yao J. Numerical simulation of microstructure evolution during laser directed energy deposition for Inconel 718 using cellular automaton method coupled with Eulerian multiphase. Int. J Heat Mass Transf 2023:216. https://doi.org/10.1016/j.ijheatmasstransfer.2023.124554.
[28] Zhang Z, Wang Y, Ge P, Wu T. A review on modelling and simulation of laser additive manufacturing: heat transfer. Microstructure Evolutions and Mechanical Properties Coatings 2022:12. https://doi.org/10.3390/coatings12091277.
[29] Singh P, M.Singari R, Mishra RS.. A review of study on modeling and simulation of additive manufacturing processes. Mater Today Proc 2022;56:3594–603. https://doi.org/10.1016/j.matpr.2021.12.057.
[30] Bayat M, Dong W, Thorborg J, To AC, Hattel JH. A review of multi-scale and multi-physics simulations of metal additive manufacturing processes with focus on modeling strategies. Addit Manuf 2021:47. https://doi.org/10.1016/j.addma.2021.102278.
[31] Poggi M, Atzeni E, Iuliano L, Salmi A. State-of-the-art of numerical simulation of laser powder Directed Energy Deposition process. Procedia CIRPvol. 112. Elsevier B.V; 2022. p. 376–81. https://doi.org/10.1016/j.procir.2022.09.012.
[32] Hume CA, Rosen DW, Woodruff GW. Low cost numerical modeling of material jetting-based additive manuracturing. n.d.
[33] Owens JT, Das A, Bortner MJ. Accelerating heat transfer modeling in material extrusion additive manufacturing: from desktop to big area. Addit Manuf 2022:55. https://doi.org/10.1016/j.addma.2022.102853.
[34] Mostafaei A, Elliott AM, Barnes JE, Li F, Tan W, Cramer CL, et al. Binder jet 3D printing—process parameters, materials, properties, modeling, and challenges. Prog Mater Sci 2021:119. https://doi.org/10.1016/j.pmatsci.2020.100707.
[35] Francois MM, Sun A, King WE, Henson NJ, Tourret D, Bronkhorst CA, et al. Modeling of additive manufacturing processes for metals: challenges and opportunities. Curr Opin Solid State Mater Sci 2017;21:198–206. https://doi.org/10.1016/j.cossms.2016.12.001.
[36] Luo Z, Zhao Y. A survey of finite element analysis of temperature and thermal stress fields in powder bed fusion additive manufacturing. Addit Manuf 2018;21:318–32. https://doi.org/10.1016/j.addma.2018.03.022.
[37] Bandyopadhyay A, Traxel KD. Invited review article: metal-additive manufacturing—modeling strategies for application-optimized designs. Addit Manuf 2018;22:758–74. https://doi.org/10.1016/j.addma.2018.06.024.
[38] Bikas H, Stavropoulos P, Chryssolouris G. Additive manufacturing methods and modeling approaches: a critical review. Int J Adv Manuf Technol 2016;83:389–405. https://doi.org/10.1007/s00170-015-7576-2.
[39] Nabavi SF, Dalir H, Farshidianfar A. A comprehensive review of recent advances in laser powder bed fusion characteristics modeling: metallurgical and defects. Int J Adv Manuf Technol 2024. https://doi.org/10.1007/s00170-024-13491-1.
[40] Jia Y, Naceur H, Saadlaoui Y, Dubar L, Bergheau JM. A comprehensive comparison of modeling strategies and simulation techniques applied in powder-based metallic additive manufacturing processes. J Manuf Process 2024;110:1–29. https://doi.org/10.1016/j.jmapro.2023.12.048.
[41] Horr AM. Real-time modelling and ML data training for digital twinning of additive manufacturing Processesa? BHM Berg- Und Hüttenmännische Monatshefte 2024;169:48–56. https://doi.org/10.1007/s00501-023-01416-6.
[42] Wang Z, Yang W, Liu Q, Zhao Y, Liu P, Wu D, et al. Data-driven modeling of process, structure and property in additive manufacturing: a review and future directions. J Manuf Process 2022;77:13–31. https://doi.org/10.1016/j.jmapro.2022.02.053.
[43] Jin Z, Zhang Z, Demir K, Gu GX. Machine learning for advanced additive manufacturing. Matter 2020;3:1541–56. https://doi.org/10.1016/j.matt.2020.08.023.
[44] Fu Y, Downey ARJ, Yuan L, Zhang T, Pratt A, Balogun Y. Machine learning algorithms for defect detection in metal laser-based additive manufacturing: a review. J Manuf Process 2022;75:693–710. https://doi.org/10.1016/j.jmapro.2021.12.061.
[45] Wang C, Tan XP, Tor SB, Lim CS. Machine learning in additive manufacturing: state-of-the-art and perspectives. Addit Manuf 2020:36. https://doi.org/10.1016/j.addma.2020.101538.
[46] Qin J, Hu F, Liu Y, Witherell P, Wang CCL, Rosen DW, et al. Research and application of machine learning for additive manufacturing. Addit Manuf 2022:52. https://doi.org/10.1016/j.addma.2022.102691.
[47] Kouraytem N, Li X, Tan W, Kappes B, Spear AD. Modeling process-structure-property relationships in metal additive manufacturing: a review on physics-driven versus data-driven approaches. JPhys Materials 2021:4. https://doi.org/10.1088/2515-7639/abca7b.
[48] Haghighi A, Li L. A hybrid physics-based and data-driven approach for characterizing porosity variation and filament bonding in extrusion-based additive manufacturing. Addit Manuf 2020:36. https://doi.org/10.1016/j.addma.2020.101399.
[49] Zhuang JR, Lee YT, Hsieh WH, Yang AS. Determination of melt pool dimensions using DOE-FEM and RSM with process window during SLM of Ti6Al4V powder. Opt Laser Technol 2018;103:59–76. https://doi.org/10.1016/j.optlastec.2018.01.013.
[50] Wang K, Zeng M, Wang J, Shang W, Zhang Y, Luo T, et al. When physics-informed data analytics outperforms black-box machine learning: a case study in thickness control for additive manufacturing. Digital Chemical Engineering 2023;6:100076. https://doi.org/10.1016/j.dche.2022.100076.
[51] Bevans BD, Carrington A, Riensche A, Tenequer A, Barrett C, Halliday H, et al. Digital twins for rapid in-situ qualification of part quality in laser powder bed fusion additive manufacturing. Addit Manuf 2024:93. https://doi.org/10.1016/j.addma.2024.104415.
[52] Guo S, Agarwal M, Cooper C, Tian Q, Gao RX, Guo WG, et al. Machine learning for metal additive manufacturing: towards a physics-informed data-driven paradigm. J Manuf Syst 2022;62:145–63. https://doi.org/10.1016/j.jmsy.2021.11.003.
[53] Ko H, Lu Y, Yang Z, Ndiaye NY, Witherell P. A framework driven by physics-guided machine learning for process-structure-property causal analytics in additive manufacturing. J Manuf Syst 2023;67:213–28. https://doi.org/10.1016/j.jmsy.2022.09.010.
[54] Wang F, Zhi Q, Zhao Z, Zhai Z, Liu Y, Xi H, et al. Inherently interpretable physics-informed neural network for battery modeling and prognosis. IEEE Trans Neural Netw Learn Syst 2023. https://doi.org/10.1109/TNNLS.2023.3329368.
[55] Ramabathiran AA, Ramachandran P. SPINN: sparse, physics-based, and partially interpretable neural networks for PDEs. J Comput Phys 2021:445. https://doi.org/10.1016/j.jcp.2021.110600.
[56] Ranasinghe N, Xia Y, Seneviratne S, Halgamuge S. GINN-KAN: Interpretability pipelining with applications in Physics Informed Neural Networks. 2024.
[57] Farrag A, Yang Y, Cao N, Won D, Jin Y. Physics-informed machine learning for metal additive manufacturing. Progress in Additive Manufacturing 2024. https://doi.org/10.1007/s40964-024-00612-1.
[58] Parsazadeh M, Sharma S, Dahotre N. Towards the next generation of machine learning models in additive manufacturing: a review of process dependent material evolution. Prog Mater Sci 2023:135. https://doi.org/10.1016/j.pmatsci.2023.101102.
[59] Sharma R, Guo YB. Computational modeling and physics-informed machine learning of metal additive manufacturing: state-of-the-art and future perspective. In: Annual Review of Heat Transfer. vol. 24. Begell House Inc.; 2022. p. 303–37. https://doi.org/10.1615/ANNUALREVHEATTRANSFER.2022041733.
[60] Guo S, Agarwal M, Cooper C, Tian Q, Gao RX, Guo WG, et al. Machine learning for metal additive manufacturing: towards a physics-informed data-driven paradigm. J Manuf Syst 2022;62:145–63. https://doi.org/10.1016/j.jmsy.2021.11.003.
[61] Mozaffar M, Liao S, Xie X, Saha S, Park C, Cao J, et al. Mechanistic artificial intelligence (mechanistic-AI) for modeling, design, and control of advanced

manufacturing processes: current state and perspectives. J Mater Process Technol 2022:302. https://doi.org/10.1016/j.jmatprotec.2021.117485.
[62] Pérez M, Carou D, Rubio EM, Teti R. Current advances in additive manufacturing. In: Procedia CIRP. vol. 88. Elsevier B.V.; 2020. p. 439–44. https://doi.org/10.1016/j.procir.2020.05.076.
[63] John Solomon I, Sevvel P, Gunasekaran J, Tanushkumaar P. A review on additive manufacturing of alloys using laser metal deposition. Mater Today Proc 2022;64: 44–50. https://doi.org/10.1016/j.matpr.2022.03.510.
[64] Özel T, Shokri H, Loizeau R. A review on wire-fed directed energy deposition based metal additive manufacturing. Journal of Manufacturing and Materials Processing 2023:7. https://doi.org/10.3390/jmmp7010045.
[65] Ahn DG. Directed energy deposition (DED) process: state of the art. International Journal of Precision Engineering and Manufacturing - Green Technology 2021;8: 703–42. https://doi.org/10.1007/s40684-020-00302-7.
[66] Kristiawan RB, Imaduddin F, Ariawan D, Ubaidillah Arifin Z. A review on the fused deposition modeling (FDM) 3D printing: filament processing, materials, and printing parameters. Open Engineering 2021;11:639–49. https://doi.org/10.1515/eng-2021-0063.
[67] Krishnanand, Taufik M. Fused Filament Fabrication (FFF) Based 3D printer and its design: A review. Lecture notes in mechanical engineering, Springer Science and Business Media Deutschland GmbH; 2021, p. 497–505. doi:https://doi.org/10.1007/978-981-15-9853-1_41.
[68] Kwon HJ, Hong J, Nam SY, Choi HH, Li X, Jeong YJ, et al. Overview of recent progress in electrohydrodynamic jet printing in practical printed electronics: focus on the variety of printable materials for each component. Mater Adv 2021; 2:5593–615. https://doi.org/10.1039/d1ma00463h.
[69] Oleff A, Küster B, Stonis M, Overmeyer L. Process monitoring for material extrusion additive manufacturing: a state-of-the-art review. Progress in Additive Manufacturing 2021;6:705–30. https://doi.org/10.1007/s40964-021-00192-4.
[70] Elkaseer A, Chen KJ, Janhsen JC, Refle O, Hagenmeyer V, Scholz SG. Material jetting for advanced applications: a state-of-the-art review, gaps and future directions. Addit Manuf 2022:60. https://doi.org/10.1016/j.addma.2022.103270.
[71] Dejene ND, Lemu HG. Current status and challenges of powder bed fusion-based metal additive manufacturing. Literature Review Metals (Basel) 2023:13. https://doi.org/10.3390/met13020424.
[72] Gao B, Zhao H, Peng L, Sun Z. A review of research progress in selective laser melting (SLM). Micromachines (Basel) 2023:14. https://doi.org/10.3390/mi14010057.
[73] Gupta R, Dalakoti M, Narasimhulu A. A Critical Review of Process Parameters in Laminated Object Manufacturing Process. 2020. p. 31–9. https://doi.org/10.1007/978-981-15-4331-9_3.
[74] Zhang F, Zhu L, Li Z, Wang S, Shi J, Tang W, et al. The recent development of vat photopolymerization: a review. Addit Manuf 2021:48. https://doi.org/10.1016/j.addma.2021.102423.
[75] ISRL book n.d.
[76] Qi X, Chen G, Li Y, Cheng X, Li C. Applying neural-network-based machine learning to additive manufacturing: current applications, challenges, and future perspectives. Engineering 2019;5:721–9. https://doi.org/10.1016/j.eng.2019.04.012.
[77] Khanzadeh M, Rao P, Jafari-Marandi R, Smith BK, Tschopp MA, Bian L. Quantifying geometric accuracy with unsupervised machine learning: using self-organizing map on fused filament fabrication additive manufacturing parts. J Manuf Sci E T ASME 2018:140. https://doi.org/10.1115/1.4038598.
[78] Tavanaei A, Ghodrati M, Kheradpisheh SR, Masquelier T, Maida A. Deep learning in spiking neural networks. Neural Netw 2019;111:47–63. https://doi.org/10.1016/j.neunet.2018.12.002.
[79] Seo J, Rao P, Raeymaekers B. Generating synthetic as-built additive manufacturing surface topography using progressive growing generative adversarial networks. Friction 2023. https://doi.org/10.1007/s40544-023-0826-7.
[80] Tan Y, Jin B, Nettekoven A, Chen Y, Yue Y, Topcu U, et al. An encoder-decoder based approach for anomaly detection with application in additive manufacturing. In: Proceedings - 18th IEEE international conference on machine learning and applications, ICMLA 2019. Institute of Electrical and Electronics Engineers Inc.; 2019. p. 1008–15. https://doi.org/10.1109/ICMLA.2019.00171.
[81] Sofi AR, Ravani B. Sub-second prediction of the heatmap of powder-beds in additive manufacturing using deep encoder–decoder convolutional neural networks. J Comput Inf Sci Eng 2023:23. https://doi.org/10.1115/1.4054559.
[82] Mahmood MA, Visan AI, Ristoscu C, Mihailescu IN. Artificial neural network algorithms for 3D printing. Materials 2021;14:1–29. https://doi.org/10.3390/ma14010163.
[83] Valizadeh M, Wolff SJ. Convolutional neural network applications in additive manufacturing: a review. Advances in industrial and manufacturing. Engineering 2022:4. https://doi.org/10.1016/j.aime.2022.100072.
[84] Zhou J, Cui G, Hu S, Zhang Z, Yang C, Liu Z, et al. Graph neural networks: a review of methods and applications. AI Open 2020;1:57–81. https://doi.org/10.1016/j.aiopen.2021.01.001.
[85] Du Y, Mukherjee T, DebRoy T. Physics-informed machine learning and mechanistic modeling of additive manufacturing to reduce defects. Appl Mater Today 2021:24. https://doi.org/10.1016/j.apmt.2021.101123.
[86] Mondal B, Mukherjee T, DebRoy T. Crack free metal printing using physics informed machine learning. Acta Mater 2022:226. https://doi.org/10.1016/j.actamat.2021.117612.
[87] Kats D, Wang Z, Gan Z, Liu WK, Wagner GJ, Lian Y. A physics-informed machine learning method for predicting grain structure characteristics in directed energy deposition. Comput Mater Sci 2022:202. https://doi.org/10.1016/j.commatsci.2021.110958.
[88] Liu R, Liu S, Zhang X. A physics-informed machine learning model for porosity analysis in laser powder bed fusion additive manufacturing. Int J Adv Manuf Technol 2021;113:1943–58. https://doi.org/10.1007/s00170-021-06640-3.
[89] Stump B. An algorithm for physics informed scan path optimization in additive manufacturing. Comput Mater Sci 2022:212. https://doi.org/10.1016/j.commatsci.2022.111566.
[90] Wang L, Zhu S-P, Luo C, Liao D, Wang Q. Physics-guided machine learning frameworks for fatigue life prediction of AM materials. Int J Fatigue 2023;172: 107658. https://doi.org/10.1016/j.ijfatigue.2023.107658.
[91] Zhao M, Wei H, Mao Y, Zhang C, Liu T, Liao W. Predictions of additive manufacturing process parameters and molten pool dimensions with a physics-informed deep learning model. Engineering 2023. https://doi.org/10.1016/j.eng.2022.09.015.
[92] Guo L, Liu H, Wang H, Cristino VAM, Kwok CT, Wei Q, et al. Deepening the scientific understanding of different phenomenology in laser powder bed fusion by an integrated framework. Int J Heat Mass Transf 2023:216. https://doi.org/10.1016/j.ijheatmasstransfer.2023.124596.
[93] Riensche AR, Bevans BD, King G, Krishnan A, Cole KD, Rao P. Predicting meltpool depth and primary dendritic arm spacing in laser powder bed fusion additive manufacturing using physics-based machine learning. Mater Des 2024:237. https://doi.org/10.1016/j.matdes.2023.112540.
[94] Smoqi Z, Gaikwad A, Bevans B, Kobir MH, Craig J, Abul-Haj A, et al. Monitoring and prediction of porosity in laser powder bed fusion using physics-informed meltpool signatures and machine learning. J Mater Process Technol 2022:304. https://doi.org/10.1016/j.jmatprotec.2022.117550.
[95] Zhang Y, Hong GS, Ye D, Zhu K, Fuh JYH. Extraction and evaluation of melt pool, plume and spatter information for powder-bed fusion AM process monitoring. Mater Des 2018;156:458–69. https://doi.org/10.1016/j.matdes.2018.07.002.
[96] Xie X, Bennett J, Saha S, Lu Y, Cao J, Liu WK, et al. Mechanistic data-driven prediction of as-built mechanical properties in metal additive manufacturing. NPJ Comput Mater 2021:7. https://doi.org/10.1038/s41524-021-00555-z.
[97] Gaikwad A, Giera B, Guss GM, Forien JB, Matthews MJ, Rao P. Heterogeneous sensing and scientific machine learning for quality assurance in laser powder bed fusion – a single-track study. Addit Manuf 2020:36. https://doi.org/10.1016/j.addma.2020.101659.
[98] Ren Y, Wang Q, Michaleris P. A physics-informed two-level machine-learning model for predicting melt-pool size in laser powder bed fusion. Journal of Dynamic Systems, Measurement and Control, Transactions of the ASME 2021: 143. https://doi.org/10.1115/1.4052245.
[99] Wenzel S, Slomski-Vetter E, Melz T. Optimizing system reliability in additive manufacturing using physics-informed machine learning. Machines 2022:10. https://doi.org/10.3390/machines10070525.
[100] Wang H, Li B, Xuan FZ. A dimensionally augmented and physics-informed machine learning for quality prediction of additively manufactured high-entropy alloy. J Mater Process Technol 2022:307. https://doi.org/10.1016/j.jmatprotec.2022.117637.
[101] Mu H, He F, Yuan L, Hatamian H, Commins P, Pan Z. Online distortion simulation using generative machine learning models: a step toward digital twin of metallic additive manufacturing. J Ind Inf Integr 2024:38. https://doi.org/10.1016/j.jii.2024.100563.
[102] Lei R, Guo YB, Guo W “Grace”. Physics-guided long short-term memory networks for emission prediction in laser powder bed fusion. J Manuf Sci Eng 2024:146. https://doi.org/10.1115/1.4063270.
[103] Cao X, Duan C, Luo X, Zheng S, Hao X, Shang D, et al. Physics-informed machine learning approach for molten pool morphology prediction and process evaluation in directed energy deposition of 12CrNi2 alloy steel. J Manuf Process 2024;119: 806–26. https://doi.org/10.1016/j.jmapro.2024.04.023.
[104] Faegh M, Haghighi A. Generative adversarial networks with domain knowledge fusion for metal additive manufacturing. Proceedings of the ASME 2024 19th international manufacturing science and engineering conference MSEC2024, Knoxville, Tennessee: ASME; 2024.
[105] Chen M, “Grace” Guo W. DCGAN-CNN with physical constraints for porosity prediction in laser metal deposition with unbalanced data. Manuf Lett 2023;35: 1146–54. https://doi.org/10.1016/j.mfglet.2023.08.116.
[106] Cooper C, Zhang J, Huang J, Bennett J, Cao J, Gao RX. Tensile strength prediction in directed energy deposition through physics-informed machine learning and Shapley additive explanations. J Mater Process Technol 2023:315. https://doi.org/10.1016/j.jmatprotec.2023.117908.
[107] Ackermann M, Haase C. Machine learning-based identification of interpretable process-structure linkages in metal additive manufacturing. Addit Manuf 2023; 71:103585. https://doi.org/10.1016/j.addma.2023.103585.
[108] Mosallanejad MH, Gashmard H, Javanbakht M, Niroumand B, Saboori A. A novel feature engineering approach for predicting melt pool depth during LPBF by machine learning models. Additive Manufacturing Letters 2024:10. https://doi.org/10.1016/j.addlet.2024.100214.
[109] Guo W “Grace”, Tian Q, Guo S, Guo Y. A physics-driven deep learning model for process-porosity causal relationship and porosity prediction with interpretability in laser metal deposition. CIRP Annals 2020;69:205–8. https://doi.org/10.1016/j.cirp.2020.04.049.
[110] Gawade V, Singh V, Guo W “Grace”. Leveraging simulated and empirical data-driven insight to supervised-learning for porosity prediction in laser metal deposition. J Manuf Syst 2022;62:875–85. https://doi.org/10.1016/j.jmsy.2021.07.013.

[111] Oikonomou A, Loutas T, Fan D, Garmulewicz A, Nounesis G, Chaudhuri S, et al. Physics-informed Bayesian learning of electrohydrodynamic polymer jet printing dynamics. n.d.

[112] Cleeman J, Agrawala K, Nastarowicz E, Malhotra R. Partial-physics-informed multi-fidelity modeling of manufacturing processes. J Mater Process Technol 2023:320. https://doi.org/10.1016/j.jmatprotec.2023.118125.

[113] Tao Z, Thanki A, Goossens L, Witvrouw A, Vrancken B, Dewulf W. Enhancing keyhole porosity detection in laser powder bed fusion using a hybrid approach of machine learning and physics-informed knowledge. n.d.

[114] Wang H, Li B, Xuan FZ. Fatigue-life prediction of additively manufactured metals by continuous damage mechanics (CDM)-informed machine learning with sensitive features. Int J Fatigue 2022:164. https://doi.org/10.1016/j.ijfatigue.2022.107147.

[115] Zamiela C, Stokes R, Tian W, Doude H, Priddy MW, Bian L. Physics-informed approximation of internal thermal history for surface deformation predictions in wire arc directed energy deposition. J Manuf Sci Eng 2024:146. https://doi.org/10.1115/1.4065416.

[116] Li Y, Mojumder S, Lu Y, Al Amin A, Guo J, Xie X, et al. Statistical parameterized physics-based machine learning digital shadow models for laser powder bed fusion process. Addit Manuf 2024:87. https://doi.org/10.1016/j.addma.2024.104214.

[117] Paulson NH, Gould B, Wolff SJ, Stan M, Greco AC. Correlations between thermal history and keyhole porosity in laser powder bed fusion. Addit Manuf 2020:34. https://doi.org/10.1016/j.addma.2020.101213.

[118] Ghungrad S, Gould B, Soltanalian M, Wolff SJ, Haghighi A. Model-based deep learning for additive manufacturing: new frontiers and applications. Manuf Lett 2021;29:94–8. https://doi.org/10.1016/j.mfglet.2021.07.008.

[119] Ghungrad S, Gould B, Wolff S, Haghighi A. Physics-informed artificial intelligence for temperature prediction in metal additive manufacturing: a comparative study. n.d. doi:https://doi.org/10.1115/MSEC2022-85159.

[120] Ghungrad S, Faegh M, Gould B, Wolff SJ, Haghighi A. Architecture-Driven Physics-Informed Deep Learning for Temperature Prediction in Laser Powder Bed Fusion Additive Manufacturing With Limited Data. J Manuf Sci Eng 2023;145: 081007 (1-11).

[121] Nagarajan HPN, Mokhtarian H, Jafarian H, Dimassi S, Bakrani-Balani S, Hamedi A, et al. Knowledge-based design of artificial neural network topology for additive manufacturing process modeling: a new approach and case study for fused deposition modeling. Journal of Mechanical Design, Transactions of the ASME 2019:141. https://doi.org/10.1115/1.4042084.

[122] Inyang-Udoh U, Mishra S. A physics-guided neural network dynamical model for droplet-based additive manufacturing. IEEE Trans Control Syst Technol 2022;30: 1863–75. https://doi.org/10.1109/TCST.2021.3128422.

[123] Xue T, Gan Z, Liao S, Cao J. Physics-embedded graph network for accelerating phase-field simulation of microstructure evolution in additive manufacturing. NPJ Comput Mater 2022:8. https://doi.org/10.1038/s41524-022-00890-9.

[124] Zhang J, Wang P, Gao RX. Attention mechanism-incorporated deep learning for AM part quality prediction. In: Procedia CIRP. vol. 93. Elsevier B.V.; 2020. p. 96–101. https://doi.org/10.1016/j.procir.2020.04.051.

[125] Mozaffar M, Liao S, Lin H, Ehmann K, Cao J. Geometry-agnostic data-driven thermal modeling of additive manufacturing processes using graph neural networks. Addit Manuf 2021:48. https://doi.org/10.1016/j.addma.2021.102449.

[126] Hershey JR, Le Roux J, Weninger F. Deep unfolding: model-based inspiration of novel deep architectures. 2014.

[127] Chien JT, Lee CH. Deep unfolding for topic models. IEEE Trans Pattern Anal Mach Intell 2018;40:318–31. https://doi.org/10.1109/TPAMI.2017.2677439.

[128] Battaglia PW, Hamrick JB, Bapst V, Sanchez-Gonzalez A, Zambaldi V, Malinowski M, et al. Relational inductive biases, deep learning, and graph networks. 2018.

[129] Coatanéa E, Roca R, Mokhtarian H, Mokammel F, Ikkala K. A conceptual modeling and simulation framework for system design. Comput Sci Eng 2016;18: 42–52.

[130] Ko H, Witherell P, Lu Y, Kim S, Rosen DW. Machine learning and knowledge graph based design rule construction for additive manufacturing. Addit Manuf 2021:37. https://doi.org/10.1016/j.addma.2020.101620.

[132] Liao S, Xue T, Jeong J, Webster S, Ehmann K, Cao J. Hybrid thermal modeling of additive manufacturing processes using physics-informed neural networks for temperature prediction and parameter identification. Comput Mech 2023. https://doi.org/10.1007/s00466-022-02257-9.

[133] Sharma R, Raissi M, Guo Y. Physics-informed deep learning of gas flow-melt pool multi-physical dynamics during powder bed fusion. CIRP Annals 2023. https://doi.org/10.1016/j.cirp.2023.04.005.

[134] Jiang F, Xia M, Hu Y. Physics-informed machine learning for accurate prediction of temperature and melt pool dimension in metal additive manufacturing. 3D Print Addit Manuf 2023. https://doi.org/10.1089/3dp.2022.0363.

[135] Tod G, Ompusunggu AP, Struyf G, Pipeleers G, Grave K De, Hostens E. Physics-Informed Neural Networks (PINNs) for Improving a Thermal Model in Stereolithography Applications. In: Procedia CIRP. vol. 104. Elsevier B.V.; 2021. p. 1559–64. https://doi.org/10.1016/j.procir.2021.11.263.

[136] Li S, Wang G, Di Y, Wang L, Wang H, Zhou Q. A physics-informed neural network framework to predict 3D temperature field without labeled data in process of laser metal deposition. Eng Appl Artif Intel 2023;120:105908. https://doi.org/10.1016/j.engappai.2023.105908.

[137] Yeh HP, Bayat M, Arzani A, Hattel JH. Accelerated process parameter selection of polymer-based selective laser sintering via hybrid physics-informed neural network and finite element surrogate modelling. App Math Model 2024;130: 693–712. https://doi.org/10.1016/j.apm.2024.03.030.

[138] Uhrich B, Pfeifer N, Schäfer M, Theile O, Rahm E. Physics-informed deep learning to quantify anomalies for real-time fault mitigation in 3D printing. Applied Intelligence 2024. https://doi.org/10.1007/s10489-024-05402-4.

[139] Zhu Q, Liu Z, Yan J. Machine learning for metal additive manufacturing: predicting temperature and melt pool fluid dynamics using physics-informed neural networks. Comput Mech 2021;67:619–35. https://doi.org/10.1007/s00466-020-01952-9.

[140] Xie J, Chai Z, Xu L, Ren X, Liu S, Chen X. 3D temperature field prediction in direct energy deposition of metals using physics informed neural network. Int J Adv Manuf Technol 2022;119:3449–68. https://doi.org/10.1007/s00170-021-08542-w.

[141] Hosseini E, Gh Ghanbari P, Müller O, Molinaro R, Mishra S. Physics informed neural networks for thermal analysis of laser powder bed fusion process. n.d.

[142] Hosseini E, Scheel P, Müller O, Molinaro R, Mishra S. Single-track thermal analysis of laser powder bed fusion process: parametric solution through physics-informed neural networks. Comput Methods Appl Mech Eng 2023:410. https://doi.org/10.1016/j.cma.2023.116019.

[143] Pierce J, Williams G, Simpson TW, Meisel NA, Mccomb C. Draft: Stochastically-trained physics-informed neural networks: Application to thermal analysis in metal laser powder bed fusion. n.d.

[144] Chen J, Pierce J, Williams G, Simpson TW, Meisel N, Prabha Narra S, et al. Accelerating thermal simulations in additive manufacturing by training physics-informed neural networks with randomly synthesized data. J Comput Inf Sci Eng 2024:24. https://doi.org/10.1115/1.4062852.

[145] Kapusuzoglu B, Mahadevan S. Physics-informed and hybrid machine learning in additive manufacturing: application to fused filament Fabrication. JOM 2020;72: 4695–705. https://doi.org/10.1007/s11837-020-04438-4.

[146] Wang H, Li B, Lei L, Xuan F. Uncertainty-aware fatigue-life prediction of additively manufactured Hastelloy X superalloy using a physics-informed probabilistic neural network. Reliab Eng Syst Saf 2024:243. https://doi.org/10.1016/j.ress.2023.109852.

[147] McGowan E, Gawade V, Guo W. A physics-informed convolutional neural network with custom loss functions for porosity prediction in laser metal deposition. Sensors 2022:22. https://doi.org/10.3390/s22020494.

[148] Zhu Q, Lu Z, Hu Y. A reality-augmented adaptive physics informed machine learning method for efficient heat transfer prediction in laser melting. J Manuf Process 2024;124:444–57. https://doi.org/10.1016/j.jmapro.2024.06.010.

[149] Sharma R, Grace Guo W, Raissi M, Guo YB. Physics-Informed Machine Learning of Argon Gas-Driven Melt Pool Dynamics. n.d.

[150] Ciampaglia A, Tridello A, Paolino DS, Berto F. Data driven method for predicting the effect of process parameters on the fatigue response of additive manufactured AlSi10Mg parts. Int J Fatigue 2023:170. https://doi.org/10.1016/j.ijfatigue.2023.107500.

[151] Salvati E, Tognan A, Laurenti L, Pelegatti M, de Bona F. A defect-based physics-informed machine learning framework for fatigue finite life prediction in additive manufacturing. Mater Des 2022:222. https://doi.org/10.1016/j.matdes.2022.111089.

[152] Baydin AG, Pearlmutter BA, Radul AA, Siskind JM. Automatic differentiation in machine learning: A survey. 2015.

[153] Zhu Q, Lu Z, Hu Y. A reality-augmented adaptive physics informed machine learning method for efficient heat transfer prediction in laser melting. J Manuf Process 2024;124:444–57. https://doi.org/10.1016/j.jmapro.2024.06.010.

[154] Gaikwad A, Yavari R, Montazeri M, Cole K, Bian L, Rao P. Toward the digital twin of additive manufacturing: integrating thermal simulations, sensing, and analytics to detect process faults. IISE Trans 2020;52:1204–17. https://doi.org/10.1080/24725854.2019.1701753.

[155] Bevans B, Barrett C, Spears T, Gaikwad A, Riensche A, Smoqi Z, et al. Heterogeneous sensor data fusion for multiscale, shape agnostic flaw detection in laser powder bed fusion additive manufacturing. Virtual Phys Prototyp 2023:18. https://doi.org/10.1080/17452759.2023.2196266.

[156] Sajadi P, Rahmani Dehaghani M, Tang Y, Wang GG. Physics-informed online learning for temperature prediction in metal AM. Materials 2024:17. https://doi.org/10.3390/ma17133306.

[157] Liu N, Li X, Rajanna MR, Reutzel EW, Sawyer B, Rao P, et al. Deep Neural Operator Enabled Digital Twin Modeling for Additive Manufacturing. 2024.

[158] Li Z, Zheng H, Kovachki N, Jin D, Chen H, Liu B, et al. Physics-informed neural operator for learning partial differential equations. n.d.

[159] Zhao Z, Ding X, Prakash BA. Pinnsformer: A Transformer-Based Frame-Work For Physics-Informed Neural Networks. n.d.

[160] Smith LN. A disciplined approach to neural network hyper-parameters: Part 1 – learning rate, batch size, momentum, and weight decay. 2018.

[161] Liao S, Xue T, Jeong J, Webster S, Ehmann K, Cao J. Hybrid thermal modeling of additive manufacturing processes using physics-informed neural networks for temperature prediction and parameter identification. Comput Mech 2023;72: 499–512. https://doi.org/10.1007/s00466-022-02257-9.

[162] Khan S, Masood Z, Usama M, Kostas K, Kaklis P, Wei, et al. Physics-Informed Geometric Operators to Support Surrogate, Dimension Reduction and Generative Models for Engineering Design. 2024.

[163] Wu G, Yion WTG, Dang KLNQ, Wu Z. Physics-informed machine learning for MPC: application to a batch crystallization process. Chemical Engineering Research and Design 2023;192:556–69. https://doi.org/10.1016/j.cherd.2023.02.048.

[164] Zhang Y, Shen S, Li H, Hu Y. Review of in situ and real-time monitoring of metal additive manufacturing based on image processing. Int J Adv Manuf Technol 2022;123:1–20. https://doi.org/10.1007/s00170-022-10178-3.

[165] Hertlein N, Buskohl PR, Gillman A, Vemaganti K, Anand S. ScienceDirect generative adversarial network for early-stage design flexibility in topology optimization for additive manufacturing. 2019.
[166] Joshi MS. Variational inference for morphological modification to 3D geometry: An application to the support generation for metal additive manufacturing. 2021.
[167] Ramlatchan A, Li Y. Image Synthesis Using Conditional GANs for Selective Laser Melting Additive Manufacturing. Proceedings of the International Joint Conference on Neural Networksvol. 2022- July. Institute of Electrical and Electronics Engineers Inc.; 2022. https://doi.org/10.1109/IJCNN55064.2022.9892033.
[168] Tang Y, Rahmani Dehaghani M, Wang GG. Review of transfer learning in modeling additive manufacturing processes. Addit Manuf 2023:61. https://doi.org/10.1016/j.addma.2022.103357.
[169] Jagtap AD, Karniadakis GE. Extended physics-informed neural networks (XPINNs): A generalized space-time domain decomposition based deep learning framework for nonlinear partial differential equations. n.d.
[170] Patrick S, Nycz A, Noakes M. Reinforcement learning for generating toolpaths in additive manufacturing. n.d.
[171] Ogoke F, Farimani AB. Thermal control of laser powder bed fusion using deep reinforcement learning. Addit Manuf 2021:46. https://doi.org/10.1016/j.addma.2021.102033.
[172] Yin M, Li T, Lei H, Hu Y, Rangan S, Zhu Q. Generalizable wireless navigation through physics-informed reinforcement learning in wireless digital twin. 2023.
[173] Shi H, Zhou Y, Wu K, Chen S, Ran B, Nie Q. Physics-informed deep reinforcement learning-based integrated two-dimensional car-following control strategy for connected automated vehicles. Knowl Based Syst 2023:269. https://doi.org/10.1016/j.knosys.2023.110485.
[174] Li Y, He S, Li Y, Shi Y, Zeng Z. Federated Multi-Agent Deep Reinforcement Learning Approach via Physics-Informed Reward for Multi-Microgrid Energy Management. 2022. https://doi.org/10.1109/TNNLS.2022.3232630.
[175] Sufian A, You C, Dong M. A deep transfer learning-based edge computing method for home health monitoring. In: 2021 55th annual conference on information sciences and systems, CISS 2021. Institute of Electrical and Electronics Engineers Inc.; 2021. https://doi.org/10.1109/CISS50987.2021.9400321.
[176] Ren T, Niu J, Qiu Y. Enhancing generalization of computation offloading policies in novel mobile edge computing environments by exploiting experience utility. J Syst Archit 2022:125. https://doi.org/10.1016/j.sysarc.2022.102444.
[177] Das A, Rad P. Opportunities and challenges in explainable artificial intelligence (XAI): A survey. 2020.
[178] Roscher R, Bohn B, Duarte MF, Garcke J. Explainable Machine Learning for Scientific Insights and Discoveries. 2019. https://doi.org/10.1109/ACCESS.2020.2976199.
[179] Koeppe A, Bamer F, Selzer M, Nestler B, Markert B. Explainable artificial intelligence for mechanics: physics-explaining neural networks for constitutive models. Front Mater 2022:8. https://doi.org/10.3389/fmats.2021.824958.
[180] Hanna JM, Aguado JV, Comas-Cardona S, Askri R, Borzacchiello D. Sensitivity analysis using physics-informed neural networks. 2023.
[181] Yeganegi F, Eamaz A, Soltanalian M. Data-aware training quality monitoring and certification for reliable deep learning. 2024.